CENTER for PRODUCE SAFETY

CPS 2020 RFP
FINAL PROJECT REPORT

Project Title
Bio-based antimicrobial coatings for reducing risk of cross-contamination during harvesting

Project Period
January 1, 2021 – December 31, 2022 (extended to March 31, 2023)

Principal Investigator
Nitin Nitin, PhD
University of California, Davis
Department of Food Science and Technology
One Shields Avenue
Davis, CA 95616
T: 530-752-6208
E: nnitin@ucdavis.edu

Co-Principal Investigators
Glenn M. Young, PhD
University of California, Davis
Department of Food Science and Technology
T: 530-752-5292
E: gmyoung@ucdavis.edu

Gang Sun, PhD
University of California, Davis
Materials Science and Engineering
T: 530-752-0840
E: gysun@ucdavis.edu

Objectives

1. *Develop approaches for rapid and uniform deposition of antimicrobial food ingredient–based coatings on harvesting knives (stainless steel), harvester conveyor belts (polyethylene), and sprockets/grooves at the turning end of conveyors, and evaluate stability of antimicrobial coatings during simulated field operations.*
2. *Demonstrate antimicrobial effectiveness of the food ingredient–based coatings against a diversity of pathogens (i.e., exogenous sources and contaminated surfaces prior to coating), and evaluate the prevention of cross-contamination of fresh produce upon contact with coated surfaces as well as the overall quality of the produce upon contact.*
3. *Field-test the coating approach to demonstrate effectiveness on harvesting knives, and estimate costs of implementing this solution for harvesting knives and harvester conveyors.*

Funding for this project was provided partly through the CPS Campaign for Research.

FINAL REPORT

Abstract

Cross-contamination of fresh produce during harvesting is a major food safety risk. This risk may result due to the persistence of pathogens on harvesting equipment and food contact surfaces or the introduction of pathogens on harvesting equipment and food contact surfaces during harvest, either from the soil, humans, or other environmental factors. Incremental changes in the sanitation of harvesting equipment may not be adequate to address these risks. To address these diverse risks during harvesting, this project proposed to develop flexible antimicrobial coatings based on a combination of selected food-grade ingredients with a commonly used chlorine-based sanitizer. The central hypothesis was that selected food-grade ingredients charged with chlorine can form flexible antimicrobial coatings to prevent cross-contamination of fresh produce from both exogenous sources of pathogens, such as soil, as well as residual/persistent populations of pathogens on equipment surfaces. The specific objectives were to (a) demonstrate the effectiveness of forming antimicrobial coatings on harvester conveyor belts and cutting knives using simple spraying or dip coating methods; (b) evaluate antimicrobial and anti-biofilm activities of the coatings on selected harvesting food contact surfaces, and demonstrate the efficacy of the approach to reduce cross-contamination in a pilot-scale operation simulating harvesting conditions; and (c) field test the antimicrobial coating solution using harvesting knives to demonstrate effectiveness in reducing the buildup of microbes on harvesting knives during a shift. The success of this project will provide a novel field deployable approach to manage food safety risks during harvesting operations by effectively controlling cross-contamination risks from food contact surfaces such as harvesting knives and conveyor belts.

Background

Preventing cross-contamination of fresh produce during harvesting is a significant challenge. This cross-contamination can happen in several ways. First, the persistence of some pathogens such as *Listeria* or *Salmonella* spp. on food contact surfaces despite using standard sanitation procedures can result in continuous cross-contamination [14]. The complexity of the equipment design, such as grooves and sprockets at the turn end of the harvester conveyor belt, as well as normal wear and tear of the equipment surface may create difficulty in the sanitation of certain parts of equipment [5]. Furthermore, there are potential risks of introducing pathogens from the soil, contaminated produce or humans during harvesting [6-9]. In addition to several studies highlighting the risk of cross-contamination during harvesting in a controlled environment [10], the risk of cross-contamination has also been validated by field studies [11-14]. Thus, there is a significant need to develop and deploy control approaches to prevent cross-contamination of fresh produce during harvesting. Development of antimicrobial coatings can be one of the approaches to address this potential risk of cross-contamination. This approach would provide active and continuous sanitation of food contact surface and thus reduce the risks of cross-contamination. Therefore, the overall goal of this study was to develop an antimicrobial coating that can be translated into actual field applications. The key features for these coatings include: (a) use of food-grade compositions to reduce the regulatory barriers; (b) flexible coating approach that could be applied on diversity of shapes and materials (knifes and conveyor belts); (c) ability to coat legacy equipment without any surface modifications; (d) ability for repeated applications as even antimicrobial surfaces can be contaminated with prolong use and wear; and (e) antimicrobial stability in the presence of organic content including produce, soil and other factors.

Research Methods and Results

1. Develop approaches for rapid and uniform deposition of antimicrobial food ingredient–based coatings on harvesting knives (stainless steel), harvester conveyor belts (polyethylene), and sprockets/grooves at the turning end of conveyors and evaluate stability of antimicrobial coatings during simulated field operations.

a. Bio-Mos and beeswax-based antimicrobial coating:

Bio-Mos (commercial source of yeast cell wall particles) and the beeswax-based antimicrobial coating were formed on polypropylene (PP) coupons. The uniqueness of this approach is that the coating could be deposited easily on plastic surfaces and removed by using hot water. In our previous study, we have shown that yeast cell wall particles (YCMPs)can bind chlorine and stabilize it in the presence of high organic content [15]. Briefly, PP coupons were coated with a solution containing 5% commercial yeast cell wall particles (Bio-Mos; BM) and 10% beeswax at 70°C. Absolute ethanol was used as a solvent during the coating deposition step, and this solvent naturally evaporated during the air-drying and cooling steps. 0.2% of glycerol and 0.2% of Tween 80 were used as an emulsifier and a plasticizer, respectively. The plastic coupons were coated by dipping for 10 s, and this was repeated three times to ensure uniform deposition of coating compositions. As shown in **Figure 1a**, the average thickness of the control plastic coupons was 1.44 ± 0.03 mm, and this was increased to 1.55 ± 0.03 mm for the plastic coupons coated with a 5% Bio-Mos suspension (5% BM). Thus, the coating process results in a small increase in the thickness of the plastic surface.

The stability of the active chlorine content on the coated plastic coupons was tested after water immersion for 1, 2, 4, and 8 h. Further, this was improved by increasing the mass of Bio-Mos to 10% (10% BM) and encapsulating food-grade polymer ε-poly-L-lysine (EPL) into Bio-Mos (10% BM-EPL). These steps increase the chlorine loading in the yeast cell wall particles. The results in **Figure 1b** demonstrate that the total chlorine content of the plastic coupons decreased as a function of water immersion time. However, the encapsulation of EPL significantly ($p < 0.05$) increased the chlorine loading capacity. The 10% BM-EPL plastic coupons after 1-h chlorination resulted in a total chlorine content of 700.00 ± 43.30 nmol/cm^2. Furthermore, the 10% BM-EPL plastic coupons after 8-h immersion (408.3 ± 38.1 nmol/cm^2) had a significantly ($p < 0.05$) higher total chlorine content than the 5% BM plastic coupons before water immersion (ca. 262.5 ± 25.0 nmol/cm^2). Regardless of the coating composition, a significant fraction of active chlorine was retained on the surface of the plastic coupons after immersion in water for an extended period of time (8 h). In summary, the beeswax–yeast cell wall particle (YCWP) combination could form an antimicrobial coating enriched with chlorine on plastic surfaces.

b. Gelatin-based hydrogel coating:

A gelatin-based antimicrobial coating was developed on a stainless-steel knife [16]. Knives were purchased from a local market and brush-coated with hydrogel paint which is composed of 10% gelatin and 5% tannic acid (w/v, based on the total solid content) (**Figure 2**). The uniqueness of this approach is the formation of a paint coating on the stainless-steel surface using a food-grade protein and an antioxidant compound, tannic acid (TA). To form multilayers of the coating, the coating and the drying process were repeated up to five times. Such a coating method provided a rapid coating on the surface of the stainless-steel knife, and the coating was formed within 80 min including the drying time (**Figure 3a**). Additional layers of the coating provided increased resistance against the aqueous environment (**Figure 3b**) and the washing process with 2% NaOH (**Figure 3c**).

To chlorinate the gelatin-TA coating, NaClO solution (1.0-1.5% available chlorine) was sprayed on the coated knife for 1 min, washed twice with DW, and dried under ambient temperature. **Figure 4a** shows the active chlorine content of the coated surfaces. It was possible to deposit a significant amount of chlorine (>12 μg/cm^2) on the knife surface using the spraying method. The stability of the chlorine deposited on the gelatin-TA coated stainless-steel knife was evaluated in diverse conditions. **Figure 4b** shows the stability of chlorine on GT_5@Cl in the simulated wash water condition (COD of 2,000 mg/L). The result showed that GT_5@Cl retained 64% of the active chlorine content even after 1 h of incubation in the presence of high organic matter. **Figure 4c** shows the stability of the bound chlorine on GT_5 at different temperatures during 14 days of storage. Interestingly, no significant decrease in active chlorine content was observed until 3 days of storage at both temperatures. However, the chlorine content decreased gradually after 3 days of storage, showing similar trends at both temperatures. After 14 days of storage, about 31.8% and 22.7% of chlorine retained active on the coating at 4 and 25°C, respectively.

The rechargeability of the chlorine content on the gelatin-TA coated stainless steel knife was tested after quenching the active chlorine using diverse methods. The active chlorine was quenched by the extended storage for 2 weeks at 25°C (**Figure 5a**), exposure to high organic content (COD of 2,000 mg/L) for 8 h (**Figure 5b**), and exposure to UV-A light for 6 h (**Figure 5c**). In addition, chemical quenching was also performed using $Na_2S_2O_3$ for five repeated cycles (**Figure 5d**). Regardless of the quenching method, the gelatin-TA coating was recharged with active chlorine to its initial level. This result indicates that the gelatin-TA coating formed on the knife surface can be simply recharged by the spraying of NaClO solution. In summary, this food-grade protein coating can be rapidly deposited on a stainless-steel (SS) surface and recharged for multiple cycles of applications.

c. Zein and yeast cell (YC)-based antimicrobial coating:

To develop coatings using plant-derived proteins, zein protein was selected as a coating material. This approach was developed based on the feedback from the CPS technical team during our annual project meeting. Zein protein is an ethanol-soluble storage protein derived from corn and has been recently explored for fresh produce coatings. The zein and YC-based antimicrobial coating was formulated on SS or PP surfaces using a simple, two-step coating method. Briefly, 10% (w/v) zein solution was prepared by dissolving zein into acetic acid, followed by the addition of glycerol (5% [w/w] based on the zein content). SS or PP surfaces were coated with zein solution either by dip-coating or spread-coating method. Before the complete drying of the zein solution, chlorinated yeast cell (YC@Cl) suspensions (20% [w/v]) were sprayed on the zein layer and air-dried for 2-4 h. **Figure 6** shows the SEM images of the PP surfaces coated with zein-based antimicrobial formulations using the two-step (dipping and spraying) method described above. It was possible to observe the uniform distribution of the YC@Cl intercalated in the zein layer on the PP surfaces. Based on the cross-sectional SEM images, the thickness of the coating was ca. 58.4 ± 5.0 um.

The storage stability of the zein and YC-based antimicrobial coating formed on SS or PP was evaluated during four weeks of storage at different temperatures (4°C and RT). Initially, ca. 1.93 ± 0.23 μmol/cm^2 and 1.46 ± 0.05 μmol/cm^2 of chlorines were deposited on SS and PP surfaces, respectively (**Figure 7**). On PP surfaces, more than 68% and 50% of the chlorine contents remained active after four weeks of storage at 4°C and RT, respectively (**Figure 7a**). Similarly, on PP surfaces, more than 53% and 42% of the chlorine contents remained active after four weeks of storage at 4°C and RT, respectively (**Figure 7b**). These results indicate that zein and YC-based formulations provided a highly localized concentration of chlorine both on SS and PP surfaces that can remain active during prolonged periods of storage at different temperature conditions.

The mechanical stability of the zein and YC-based antimicrobial coating was evaluated both against dry and wet shear abrasions using the EPA-recommended sponge abrasion test for antimicrobial surfaces (**Figure 8**). Briefly, a dry or wet sponge was passed on the coated surfaces repeatedly with an additional weight of 224 g (dry abrasion) or 454 g (wet abrasion) for up to 30 cycles (dry abrasion: 1 cycle = 16 single passes; wet abrasion: 1 cycle = 8 single passes). According to the EPA guidelines, 30 cycles correspond to a 3-week duration of the antimicrobial surface under the actual processing condition. The coating formed on SS surfaces showed very strong mechanical resistance against dry and wet shear abrasions, and no significant loss of the chlorine content was observed during 30 cycles of abrasions (**Figure 8a**). On the contrary, the chlorine content of the coating formed on PP surfaces significantly decreased after 30 cycles of dry abrasion or 20 cycles of wet abrasion compared to its initial chlorine content (**Figure 8b**). However, even after 30 cycles of dry and wet abrasions, ca. 86% (1.26 μmol/cm^2) and 78% (1.14 μmol/cm^2) of the initial chlorine content still remained active on the surfaces. Based on our previous results, 0.5 μmol/cm^2 is considered a sufficient amount of chlorine that can inactivate >5 log of *Escherichia coli* O157:H7 cells within 30 min upon direct contact (data not shown). Our results demonstrated that the zein and YC-based antimicrobial coating formulated on SS or PP surfaces could endure dry and wet shear stresses that might occur in the actual fresh produce handling environments without losing its efficacy. In summary, these results illustrate significant mechanical stability in both wet and dry abrasion environments, high chlorine loading yield, and chemical stability of the chlorine bound to the zein-coated particles with the zein-based coating.

d. Gelatin and Soy Protein Hydrolysate (SPH)-based antimicrobial coating:

Following the concept of the protein-based halamine antimicrobial coating strategy, two coating deposition technologies were developed for the most commonly used plastic surfaces. Low-density polyethylene (LDPE), a representative olefin polymer widely used in food-producing industries, was employed in this study. Gelatin was used as a representative of soluble proteins.

Figure 9a illustrates the structures of proposed hydrogel antimicrobial deposition systems and their typical development–application cycle. In this cycle, LDPE is first coated with the developed systems and charged with active chlorine after drying. The charged coating performs antimicrobial function by releasing active chlorine when it encounters microorganisms or organic matter. The deposition system can undergo several charge-release cycles with sufficient active chlorine content as required. At the end of the application cycle, the deposition layer can be easily removed during standard sanitation procedures by steam or hot water flush. Two food ingredient-based coating systems were developed and compared, namely Gel/TA@LDPE and Gel/SPH/TA@LDPE, which are based on TA-crosslinked gelatin (Gel) and TA-crosslinked Gel/SPH composite networks, respectively. To prepare the coating systems, TA was mixed with protein solutions at pH 8, leading to the oxidation of the phenolic groups in TA to quinones and subsequent crosslinking of proteins (Gel or Gel and SPH) through Michael addition or Schiff base reactions, as depicted in **Figure 9b**. The protein-based hydrogel coatings can be easily functionalized with halamine groups by exposure to sodium hypochlorite or diluted Clorox solutions, as shown in **Figure 9c**. In the development of the coating systems, it is important to carefully control the degree of crosslinking for two reasons. First, the crosslinking induced by TA consumes primary amine groups in proteins, which reduces the capacity of the system to form N-halamine structure for antimicrobial functions. Additionally, the degree of crosslinking of the hydrogel network determines the stability of antimicrobial crosslinking during application and the ease of removal at the end of an application cycle.

Plasma treatment was used to modify the inherent hydrophobic nature of LDPE and facilitate the subsequent deposition of hydrophilic proteins. Contact angle measurements were taken and are presented in **Figure 10a** and **Figure 11**, revealing a sharp reduction in water-

LDPE contact angle within the first minute of plasma treatment, reaching equilibrium after 3 min. In halamine-biocidal systems, the deposition thickness plays a crucial role in determining overall charging capacity and potential antimicrobial performances. To achieve homogenous deposition with uniform thickness, a pipetting method was employed that precisely controlled the pick-up rate, where 500 µL of protein solution at 50°C was evenly distributed onto the surface of a 20 mm × 50 mm LDPE coupon (plasma-treated for 3 min). The warm protein solutions spread evenly and spontaneously due to their low viscosity at elevated temperatures. As shown in **Figure 12**, the deposition uptake rate remained at 7.5% ± 0.5% of the LDPE coupon mass, ensuring uniform deposition for subsequent tests. To mimic the application conditions, the stability of different deposition systems was tested with fully dehydrated post-coated LDPE coupons in various water-rich conditions.

The efficacy of plasma treatment in enhancing coating adhesion is demonstrated in **Figure 10b**, where untreated LDPE coupons did not display adequate adhesion to the Gel coating layer, while Gel@LDPE (10% gelatin) deposition became stable after just 10 seconds of plasma treatment. These findings are supported by the results presented in **Figure 10c**, which indicate that plasma treatment significantly improved the stability of the Gel@LDPE deposition system, with 10 to 180 seconds of plasma treatment demonstrating consistent deposition retention rates when subjected to immersion in a 4°C still water bath for 5 days or rinsed in a 4°C still water bath for 24 hours. Conversely, without plasma treatment, the coated layer rapidly peeled off upon immersion in water. To ensure optimal stability of the potential deposition layer, a 3-minute plasma treatment duration was utilized in all subsequent deposition steps.

To enhance the stability of the water-soluble protein-based deposition system in water-rich environments, tannic acid (TA), a food-grade and environmentally friendly crosslinking agent, was employed. TA crosslinks proteins through both physical and chemical crosslinks. The physical crosslinking includes hydrogen bonding and π-π stacking with the benzene rings in Phenylalanine (Phe), Tyrosine (Tyr), and Tryptophan (Trp). The covalent bond establishment between TA and proteins is pH-dependent and oxygen-sensitive, with TA transitioning from phenol to a quinone structure at pH 8, enabling Michael addition and Schiff base reactions with amine groups in protein polymeric chains, as illustrated in **Figure 9b**. The impact of TA on stability was more pronounced in the Gel/SPH-based deposition systems, as demonstrated in **Figure 10d** and **Figure 10e**, where the mass retention rates of Gel-based deposition systems remained similar regardless of the presence of TA, while the incorporation of TA in Gel/SPH-based deposition system was crucial in reducing mass loss in water-rich environments. **Figure 10e** shows that the addition of 1% TA, based on total protein content, resulted in a significant improvement in the stability of the Gel/SPH-based deposition system on 3-minute plasma-treated LDPE coupons. Further increasing the TA concentration did not result in significant improvement.

The swelling ratio of Gel-based and Gel/SPH-based deposition systems with different TA concentrations reveals the degree of crosslinking, as shown in **Figure 10f** and **Figure 10g**. The addition of 1% TA in both systems increased their degrees of crosslinking and reduced the swelling ratio, which is consistent with stability test results. However, increasing the concentration of TA beyond 1% did not further increase the degree of crosslinking. Instead, when 5% TA was added, the swelling speed and swelling ratio of Gel/TA-based deposition slightly increased, indicating that the degree of crosslinking was not as effective as 1%-3% TA, possibly due to the TA aggregation. Gel/SPH-based systems with 3% TA and 5% TA exhibited similar swelling behaviors, indicating the 3% TA was efficient enough to crosslink as described in Gel/SPH-based deposition systems.

From the above test, it can be concluded that the addition of 1% TA improved the degree of crosslinking for both Gel-based and Gel/SPH-based deposition systems. The increase of crosslinking degree is important to Gel/SPH-based systems as they showed less stability compared to Gel-based systems. To ensure a fair comparison of the performance of the

two coating systems, 1% TA was added to both Gel-based and Gel/SPH-based deposition systems, and the resulted Gel/TA@LDPE (10% gelatin with 1% TA, TA concentration calculated out of total protein content) and Gel/SPH/TA@LDPE (9% gelatin, 1% SPH with 1% TA, TA concentration calculated out of total protein content) were employed in subsequent tests. The appearances of Gel/TA@LDPE and Gel/SPH/TA@LDPE are presented in **Figure 10h**. The stability of Gel/TA@LDPE and Gel/SPH/TA@LDPE was further tested in an ambient temperature water bath, and mass retention rates were measured and are shown in **Figure 10i**. The results showed that Gel/TA@LDPE retained 94.6% and 93.8% of the initial deposition mass after 2-hour and 24-hour immersion, respectively, while Gel/SPH/TA@LDPE retained 88.2% and 80.4% of the initial deposition mass after 2-hour and 24-hour immersion. The overall mass retention was satisfactory, considering that the deposition system is not expected to function under ambient temperature for extended periods in washing solutions in the fresh-produce production line. Both deposition systems remained stable with short-term exposure to water under ambient conditions.

The developed Gel/TA@LDPE and Gel/SPH/TA@LDPE are expected to show active chlorine by simply soaking the coated LDPE coupons in a diluted chlorination solution. While the intrinsic susceptibility of the proteins to oxidation prevents the use of highly concentrated chlorination solutions, 100 mL of chlorination solution with 10 ppm of free active chlorine content was used to charge one Gel/TA@LDPE-coated or Gel/SPH/TA@LDPE-coated LDPE coupon in these tests. Active chlorine contents of chlorinated deposition systems were measured via an established iodometric titration method. The chlorination efficiency was highly influenced by the pH condition of the chlorination solutions due to the different reaction activities of hypochlorous moieties ($HOCl/OCl^-$) and amine structures. At low pH values, the amino groups in proteins and the hypochlorous acid (pKa = 7.53) can be protonated, forming structures of $-NH_3^+$ and HOCl. The protonated primary amines are hard to be converted to N-halamine structure (NH-Cl), while the HOCl is more effective than ClO^- in generating N-halamine structures. It is a balance of converting between effective structures in proteins and the hypochlorous acid. As a result, Gel/TA@LDPE showed the highest ability in forming N-halamine structures at pH 3 and exhibited decreasing total active chlorine content from pH 3 to pH 12, as shown in **Figure 13a**. Although the best charging performance was obtained at pH 3 for Gel/TA@LDPE system, the harsh pH condition can cause food safety and operational concerns considering the application environment and safety requirements of the designed coating systems. Thus, pH 6 was selected for the chlorination solutions of both Gel/TA@LDPE and Gel/SPH/TA@LDPE deposition systems to achieve a satisfying chlorination level.

Figure 13b demonstrates the active chlorine content of Gel/TA@LDPE and Gel/SPH/TA@LDPE deposition systems after immersion in chlorination solutions (10 ppm, pH 6) for up to 60 minutes. Both systems showed increasing active chlorine content over time. Gel/TA@LDPE reached equilibrium after 60 minutes with 1385 ppm, while Gel/SPH/TA@LDPE reached equilibrium after 5 minutes with 800 ppm. Gel/TA@LDPE had a higher maximum capacity than Gel/SPH/TA@LDPE though it requires a longer chlorination time.

The maximum charging capacity of the Gel/TA@LDPE and Gel/SPH/TA@LDPE deposition systems for N-halamine formation depends on available precursor sites in the systems, decided by the total protein contents. Considering the potential instability of protein-based deposition systems in oxidative environments, we also measured the mass retention of both depositions systems in as mentioned chlorination solution (10 ppm, pH 6) for up to 60 minutes. **Figure 13c** indicates that Gel/TA@LDPE and Gel/SPH/TA@LDPE lost only small percentages of mass, at 2% and 10%, respectively, which is similar to the mass loss in water without free active chlorine content at ambient conditions shown in **Figure 10i**. This confirmed that the chlorination solution (10 ppm, pH 6) did not reduce the capacity of the two deposition systems, and it was feasible to continue testing the recharging performances of the deposition systems.

The stability of Gel/TA@LDPE and Gel/SPH/TA@LDPE deposition systems was evaluated by storing the coated LDPE coupons in a dark environment with 40% relative humidity at 21°C for multiple days. For a fair comparison, both deposition systems were charged in chlorination solutions (10 ppm, pH 6) for 20 min, reaching an active chlorine content of 850 ± 30 ppm. **Figure 14a** shows that Gel/SPH/TA@LDPE exhibited better retention of active chlorine against storage time compared to Gel/TA@LDPE systems. The Cl^+ content of Gel/SPH/TA@LDPE decreased from 879 ppm (day 0) to 833 ppm, 190 ppm, and 78.4 ppm after 1, 3, and 5 days of storage, respectively. On the other hand, the Cl^+ content of Gel/TA@LDPE decreased from 826 ppm (day 0) to 420 ppm after 1 day and reduced to below the detection limit after 3 days. The storage stability of both Gel/TA@LDPE and Gel/SPH/TA@LDPE was found to be limited at ambient temperature after 1 day of storage. Therefore, it is recommended to charge both deposition systems right before their intended application cycle to ensure maximum efficiency. Moreover, storing the systems at lower temperatures could potentially increase their storage stability, as oxidative degradation is known to be temperature dependent.

The reusability of the Gel/TA@LDPE and Gel/SPH/TA@LDPE coatings was further evaluated through multiple recharging cycles. As shown in **Figure 14b**, the Gel/TA@LDPE coating retained more than 95% of its initial deposition mass after 4 washing cycles, indicating good stability. Gel/SPH/TA@LDPE showed less stability, as illustrated in previous tests, and retained more than 80% of its initial deposition mass after 4 washing cycles. It is noteworthy that repeated charging cycles did not induce continuous mass losses as the mass reduction was mainly caused by the first charging cycle, for both Gel/TA@LDPE and Gel/SPH/TA@LDPE coatings.

The protein-based antimicrobial deposition systems are designed for easy removal during standard sanitation procedures. Properly controlling the degree of crosslinking resulted in both Gel/TA@LDPE and Gel/SPH/TA@LDPE exhibiting stable performance below ambient conditions while being easily removable with hot water. **Figure 14c–d** demonstrates that both coating systems can be completely removed by 50°C water. In the experiment, it was observed that keeping the coated LDPE coupons in a stirring 50°C water bath for 1 minute effectively washed off both Gel/TA@LDPE and Gel/SPH/TA@LDPE coatings. It is reasonable to predict that pressurized steam can remove the depositions even more effectively and rapidly. Furthermore, removing both depositions from LDPE requires only a small amount of water, as 1 liter of 50°C water was able to process more than 250 coated LDPE coupons, as shown in **Figure 14e**. The wastewater can be directly disposed through the sewer, as all the components are environmentally friendly and disposable.

In conclusion, the protein-based Gel/TA@LDPE and Gel/SPH/TA@LDPE deposition systems have demonstrated stable performances at and below ambient conditions, while also being easily removable by hot water or steam. These sustainable and environmentally friendly coating systems have the potential to provide effective and safe antimicrobial protection for different hydrophobic food-contacting surfaces.

2. Demonstrate antimicrobial effectiveness of the food ingredient–based coatings against a diversity of pathogens (i.e., exogenous sources and contaminated surfaces prior to coating), and evaluate the prevention of cross-contamination of fresh produce upon contact with coated surfaces as well as the overall quality of the produce upon contact.

a. Bio-Mos (BM) and beeswax-based antimicrobial coating:

The rapid antimicrobial activity of chlorine-charged 5% BM plastic coupons was demonstrated against *E. coli* O157:H7. As shown in **Figure 15**, the chlorine-charged 5% BM plastic coupons (ca. 262.5 ± 25.0 nmol/cm^2) completely inactivated *E. coli* O157:H7 by 10-min contact from the

initial inoculum of 5 log CFU/cm^2 (**Figure 15a**). **Figure 15b** shows that this level of bacterial inactivation (>4 log reduction) could be achieved within shorter treatment times (2 and 5 min).

The chlorine stability and antimicrobial activity of the coated plastic coupons were also tested in the presence of organic matter. The results in **Figure 16a** illustrate that the presence of 500 ppm COD reduced the total chlorine contents of the 5% BM and 10% BM plastic coupons from 262.5 ± 25.0 and 354.2 ± 52.0 nmol/cm^2 to 162.5 ± 25.0 and 187.5 ± 25.0 nmol/cm^2, respectively. In contrast, the total chlorine content of the 10% BM-EPL plastic coupons was 658.3 ± 80.4 nmol/cm^2 under the same condition. Moreover, the total chlorine contents of these coupons were maintained high against increased COD levels, i.e., 683.33 ± 38.19 and 558.33 ± 38.19 nmol/cm^2 in the presence of 1,000 and 20,000 ppm COD, respectively. The results in **Figure 16b** demonstrate the respective antimicrobial activity in the presence of organic matter. No bacteria were detected on the 10% BM-EPL plastic coupons in the presence of 500–20,000 ppm COD.

The cross-contamination process between fresh produce and plastic surfaces was simulated as shown in **Figure 17a**. A texture analyzer was used to precisely control the contact time (10 min) and applied contact force (1 N). The results in **Figure 17b** demonstrate that the chlorine-charged 10% BM-EPL plastic coupon could significantly ($p < 0.05$) reduce the cross-contamination from a baby spinach leaf. These results show that the bacterial transfer from a leaf contaminated with 4.68 ± 0.35 log CFU/cm^2 of *E. coli* O157:H7 was eliminated on both the coated plastic surfaces and leaves. The bacterial counts after the 2nd contact were under the detection limit in both cases.

b. Gelatin-based hydrogel coating on stainless steel coupon:

Listeria innocua and *E. coli* O157:H7 were used as model bacteria for testing antimicrobial effectiveness of chlorine charged gelatin-tannic acid hydrogel coating. The prepared antimicrobial coating on stainless steel coupons eliminated both *L. innocua* and *E. coli* O157:H7 in 5 min contact in the absence of organic matter (0 mg/L of COD; **Figure 18a and b**). The antimicrobial activity in simulated wash water condition (2,000 mg/L of COD) was also tested. As shown in **Figure 18c and d**, both *L. innocua* and *E. coli* O157:H7 were inactivated upon contact with the chlorine charged gelatin coating in the presence of organic content. The results exhibit that even 5 min of contact with the chlorine charged hydrogel coated stainless steel can effectively reduce both bacteria (>5 log CFU/cm^2 reduction) in the presence of 2,000 mg/L COD.

The anti-biofouling activity of the hydrogel coating was investigated against *L. innocua* and *E. coli* O157:H7. Both bacterial suspensions (ca. 4 - 4.5 log CFU/cm^2) were incubated at room temperature in the dark for 3 days, respectively. As shown in **Figure 19**, the chlorine-charged, gelatin-TA hydrogel coating effectively prevented both bacterial cells from biofilm formation on the stainless surfaces even after 3 days of incubation. On the other hand, significant bacterial growth was observed on the control samples (SS and GelTA), indicating the potential biofilm formation on the control surfaces.

The cross-contamination process between spinach leaf and the surface of stainless steel was simulated as described in **Figure 20a**. The result illustrated in **Figure 20b** shows that the chlorine charged Gel-TA hydrogel coating effectively prevented the leaf-surface-leaf cross-contamination of both tested bacteria (*L. innocua* and *E. coli* O157:H7). Interestingly, there were no culturable *E. coli* O157:H7 cells on the coated SS surfaces after 10 min of contact with the donor leaf (ca. 6.8 log CFU/cm^2).

c. Gelatin-based hydrogel coating on stainless steel knife:

The antimicrobial activity of GT_5@Cl was tested against the natural microflora present on the fresh Romaine lettuce. A single chopping cycle was composed of 30 cuttings of Romaine lettuce, and the test was performed for up to 5 cycles (150 cuttings). The number of bacterial

cells that are present on the GT_5@Cl surface was enumerated after each chopping cycle and compared to the control samples. Non-coated knives, G_5, and G(T)_5 were used as control samples. Non-coating, non-treatment knife (NC NT) was used as a negative control, and no colony was observed. After the first chopping cycle, ca. 3.1 log CFU/cm^2 of bacterial cells were present on GT_5@Cl surfaces, whereas ca. 5.1-5.6 log CFU/ cm^2 of bacterial cells were present on the control samples **(Figure 21a**). The bacterial cell number was measured based on an aerobic plate count assay. This indicates that there was a significant reduction of bacterial cells (ca. 2.0-2.5 log reduction) on the GT_5@Cl surfaces due to the *N*-halamines formed on the surfaces. In addition, not any additional increase in the number of bacterial cells was observed on GT_5@Cl after five cycles of chopping **(Figure 21b)**. This indicates that the GT_5@Cl can exert persistent antimicrobial activities during repetitive use.

d. Gelatin-based hydrogel coating on PP conveyor belt:

The effectiveness of the gelatin-based antimicrobial coating in preventing bacterial cross-contamination was evaluated on the actual conveyor belt surface. Briefly, 2-3 baby spinach leaves were placed on the coated or uncoated conveyor belt surface within the defined area (5 x 5 cm^2), and the bacterial cells transferred to the conveyor belt surfaces from spinach leaves after conveying cycles were enumerated using a swab-sampling method. Each conveying cycle was composed of 10 min incubation of spinach leaves on the coated or uncoated surface, and the test was performed for up to 10 conveying cycles to simulate the accumulated cross-contamination of the conveyor belt surface over repeated conveying cycles of spinach leaves. **Figure 22a** shows the experimental setup of the cross-contamination study. **Figure 22b** shows the total plate count of the natural microflora transferred to the coated or uncoated surfaces of the conveyor belt. After the first conveying cycle, ca. 2.38 ± 0.08 log CFU/unit area of microflora was transferred on the uncoated conveyor belt, and the total bacterial count accumulated up to ca. 3.29 ± 0.29 log CFU/unit area after 10 conveying cycles. In contrast, only ca. 0.85 ± 0.21 log CFU/unit area of the bacteria survived on the conveyor belt with gelatin-based coating, and the total bacterial count reached ca. 1.92 ± 0.11 log CFU/unit area after 10 conveying cycles. In addition, when the spinach leaves were kept overnight on the coated conveyor belt, no microflora was found on the coated surfaces, whereas 1.92 ± 0.11 log CFU/unit area of bacteria was enumerated from the uncoated surfaces. Our results proved that the gelatin-based antimicrobial coating formulations could be applied on the actual conveyor surfaces, lower the risk of crop-to-surface cross-contamination, and improve the microbiological safety of the fresh produce-handling environment.

e. Zein and yeast cell (YC)-based antimicrobial coating on PP coupons:

The antimicrobial activities of the zein and YC-based coating formed on PP surfaces were tested against both Gram-negative (*E. coli* O157:H7) and Gram-positive (*Listeria innocua)* model bacteria. As illustrated in **Figure 23a**, populations of *E. coli* O157:H7 cells (ca. 6.5 log CFU/cm^2) inoculated on the coated surface showed >5 log reductions within 5 min of treatment and decreased to its theoretical detection limit (1.0 log CFU/cm^2) within 10 min. Similarly, populations of *L. innocua* cells inoculated on the coated surface decreased to the theoretical detection limit within 5 min of contact (**Figure 23b**). The results indicate that the zein and YC-based coating can provide strong antimicrobial activities to the fresh produce handling surfaces against a broad spectrum of pathogens upon contact and, as a result, lower the risk of microbial contamination of the food contact surfaces.

3. Field-test the coating approach to demonstrate effectiveness on harvesting knives, and estimate costs of implementing this solution for harvesting knives and harvester conveyors.

a. Field test on a Romaine lettuce farm:

Based on the superior mechanical stability, stability of chlorine in the coating composition, and effective loading of chlorine, the zein-based coating composition was selected for field testing. In addition, the zein coating was made with plant protein-derived ingredients and thus was preferred for field testing. The zein-and YC-based antimicrobial coating was formulated on a lettuce harvesting knife using a two-step coating method and tested on a lettuce farm in San Lucas. A harvesting knife was selected as an example of extreme shear and organic content exposure to the coated surface. The field test was conducted in two different scenarios: lettuce harvesting and trimming scenarios. **Figure 24a** shows the change in active chlorine contents of the coated knife during harvesting/trimming 100 lettuce heads. The initial active chlorine content (ca. 0.314 μmol/cm^2) showed a significant ($p < 0.05$) reduction during the field operation and decreased to ca. 0.061 and 0.086 μmol/cm^2 after harvesting and trimming 100 lettuce heads, respectively. However, even after harvesting and trimming 100 heads of lettuce, ca. 20% and 28% of the chlorine still remained active on the harvesting knife, indicating the relative stability of the chlorine content bound on YC particles. This result is significant as the harvesting and trimming operations significantly expose the coating to significant organic content and mechanical shear. In the harvesting operation, the knife is in contact with the soil, while during the trimming operation, significant fraction of exudate from the lettuce heads is released. Based on the visual observation, two different sides of the harvesting knife were affected during each harvesting or trimming scenario (**Figure 24b**). It was possible to observe a loss of the coating materials on the upper side of the blades after the harvesting operation, whereas coatings on the lateral side of the blades were more affected during the trimming operation. Despite the presence of high organic load and the mechanical shear, a significant fraction of the coating was maintained on the harvesting knife surface.

The antimicrobial activities of the zein-based coating on the harvesting knife were evaluated by monitoring the accumulation of the microbial loads (total plate count [TPC], coliforms, and yeast and molds [YM]) on the surface of the coated knife during the field operation. **Figure 25** shows the accumulation of microbial loads on the lettuce harvesting knife during harvesting/trimming operations. On the control knives without antimicrobial coating, the microbial loads accumulated up to ca. 5.27 log CFU (TPC), 4.23 log CFU (coliforms), and 3.84 log CFU (YM) per unit area (1 cm^2) after harvesting 100 heads of lettuce, whereas only ca. 3.53 log CFU (TPC), 2.33 log CFU (coliforms), and 1.4 log CFU (YM) were found culturable on the coated knife. During the trimming operation, microbial loads accumulated up to ca. 4.05 log CFU (TPC), 3.39 log CFU (coliforms), and 2.88 log CFU (YM) on the uncoated knife, whereas only ca. 2.55 log CFU (TPC), 1.69 log CFU (coliforms), and 0.98 log CFU (YM) were found culturable on the coated knife. The results demonstrated that the zein and YC-based antimicrobial coating can provide antimicrobial activity in actual field operations even in the presence of harsh abrasion generated from soil and lettuce content and showed about 55-fold (TPC), 80-fold (coliforms), and 27.5-fold (YM) lower microbial accumulation after harvesting, and 32-fold (TPC), 50-fold (coliforms), and 80-fold (YM) lower microbial accumulation after trimming 100 heads of Romaine lettuce compared to the uncoated counterpart, respectively.

b. Field test in a stone fruit packing facility:

This test was designed to assess if the coating could function in a dry environment such as a packaging table for fruit packing. The zein-and YC-based antimicrobial coating was formulated on a stone fruit sorting table using a two-step coating method. Change in active chlorine content

and the accumulation of the microbial loads on the sorting table with and without antimicrobial coating were monitored during 5 h of the actual peach grading operation. **Figure 26a** shows the images of the antimicrobial coating before and after 5 h of the grading operation. Although there was some loss of coating materials after 5 h, the majority of the coating material seemed to be well-retained on the grading table. This is further supported by the active chlorine measurement. **Figure 26b** shows the change in active chlorine contents before and after the grading operation. Although the active chlorine contents showed a significant ($p < 0.05$) decrease after the grading operation, ca. 65% of the initial chlorine content still remained active on the sorting table even after 5 h of operation. The results indicate that the zein and YC-based coating has significant mechanical resistance to withstand abrasive stresses that are generated during the actual peach sorting processes.

The antimicrobial activities of the zein-based coating on a fruit grading table were evaluated by monitoring the accumulation of the microbial loads (TPC, coliforms, and YM) on the surface of fruit grading tables with and without the antimicrobial coating. As illustrated in **Figure 27a**, the microbial loads accumulated up to ca. 3.74 log CFU (TPC), 3.11 log CFU (coliforms), and 3.46 log CFU (YM) per unit area (16 cm^2) on the control surfaces without antimicrobial coating, whereas only 1.80 log CFU (TPC), 1.56 log CFU (coliforms), and 1.72 log CFU (YM) per unit area were found culturable on the coated sorting table after 5 h of the peach grading operation. Overall, the sorting table with antimicrobial coating showed about 87-fold (TPC), 36-fold (coliforms), and 112-fold (YM) lower microbial accumulation based on the plate count assay, compared to the uncoated surfaces.

Lastly, the possible adverse effects of the zein-based antimicrobial coating on fresh produce were evaluated by monitoring the residual chlorine content and color change of the peach samples. Based on the LC-MS/MS analysis, there were no chlorate (limit of detection: 10 ppb) nor perchlorate (limit of detection: 2 ppb) contents found on the peach samples after 10 min of rolling operation on the antimicrobial coating (data not shown). In addition, possible color change of the peach samples was monitored using the Hunter colorimeter (**Figure 27b**). Based on the Hunter *L, a, b* color scale, no perceptible color change ($\Delta E^*_{ab} < 2$) was observed on the peach samples even after 1 h of contact with coated surfaces. This indicates that the zein-based coating formulated on the grading table not only can persist against mechanical stresses but also reduce the microbial risk of the fruit-handling surfaces without affecting the quality of stone fruits.

c. Cost estimation of zein-based antimicrobial coating formulation:

The cost of formulating zein-based antimicrobial coating on an industrial scale was estimated using SuperPro Designer software. **Figure 28** illustrates the overall process design of the industrial-scale, zein-based coating formulation. Prices of the ingredients were estimated based on the average industrial pricing, and one batch was composed of 22 kg of the coating formulation. Overall, it was estimated that $15.60 of operating cost was required to formulate 1 kg of zein-based coating on the surface. Considering the versatility of the zein-based coating, the thickness of the coating can be adjusted to formulate a thicker (50 g coating / m^2) or thinner (50 g coating / m^2) coating on diverse surfaces depending on its application. In the case of the thicker coating, it was estimated that $0.78 is needed to coat 1 m^2 of the substrate, and $0.47 is required for depositing a thinner coating on the substrate. Among the operating costs, the cost needed for the materials ($272/batch) accounted for ca. 79.3% of the whole operating cost, followed by the labor-dependent costs ($58/batch), QC/QA ($9/batch), and utilities ($4/batch) which accounted for ca. 16.9%, 2.6%, and 1%, respectively.

Outcomes and Accomplishments

1. Beeswax and YCWP-based antimicrobial coating

- A food-grade antimicrobial coating composed of beeswax and yeast cell wall particles (YCWPs) was developed for polypropylene (PP) surfaces.
- The loading capacity and stability of active chlorine on the coating were significantly enhanced by encapsulating a food-grade biopolymer, ε-poly-L-lysine (EPL), into YCWPs.
- Rapid inactivation (<2 min) of *E. coli* O157:H7 (>4 log CFU/cm^2) was achieved on the coated PP surfaces even in the presence of high organic matter (COD 20,000 ppm).
- The coating had moderate stability in the presence of water. This instability was largely attributed to the potential phase separation of the hydrophilic yeast cells from the hydrophobic wax coating in the presence of water.
- The beeswax and YCWP-based coating formulated on PP surfaces effectively reduced the risk of leaf-surface-leaf cross-contamination of spinach leaves, and no *E. coli* O157:H7 cells were found on the recipient coated PP and leaf surfaces.

2. Gelatin-based antimicrobial coating

- A food-grade antimicrobial coating composed of gelatin and tannic acid was developed for stainless steel (SS) coupons, SS knives, and PP conveyor belts.
- SS coupons coated with gelatin-based antimicrobial formulations showed strong antimicrobial (4 log inactivation within 5 min) and antibiofilm activities against *L. innocua* and *E. coli* O157:H7 cells.
- The gelatin-based antimicrobial coating formulated on SS coupons effectively reduced the risk of leaf-surface-leaf cross-contamination of spinach leaves with *L. innocua* and *E. coli* O157:H7, respectively.
- The gelatin-based antimicrobial coating significantly reduced the microbial accumulation on the SS knife surfaces during the extensive chopping cycles for Romaine lettuce.
- The gelatin-based antimicrobial coating significantly reduced the microbial accumulation on the PP conveyor belt during simulated conveying operations of fresh spinach leaves.

3. Zein and YC-based antimicrobial coating

- A food-grade antimicrobial coating composed of zein and yeast cells (YCs) was developed for PP coupons, SS lettuce harvesting knife, and SS fruit grading table.
- PP coupons coated with zein and YC-based antimicrobial formulations showed strong antimicrobial activities and achieved >5 log reductions of *E. coli* O157:H7 and *L. innocua* cells within 5 min of contact, respectively.
- The zein and YC-based antimicrobial coating significantly reduced the microbial accumulation on the lettuce harvesting knife during harvesting and trimming 100 heads of Romaine lettuce.
- The zein and YC-based antimicrobial coating significantly reduced the microbial accumulation on the fruit sorting table during 5 hours of peach grading operations.
- The zein and YC-based antimicrobial coating did not cause any perceptible color change ($\Delta E^*_{ab} < 1$) on the peach surfaces, and no residual chlorate (< 10 ppb) or perchlorate (< 2 ppb) content was detected on the peach samples after the simulated grading operations.

Summary of Findings and Recommendations

- Rapid and uniform coating formulations were developed using food-grade biopolymers including beeswax, gelatin, gelatin/soy protein, and zein, and/or yeast-based microcarriers including YCs and YCWPs for diverse food-contact and handling surfaces.

- The mechanical stability of the coating formulations was demonstrated in the simulated processing operations.

- Rapid inactivation (<5 min) of the diverse pathogenic bacteria (*E. coli* O157:H7 and *L. innocua*) was demonstrated on diverse SS and PP surfaces in the presence of organic matter.

- SS and PP surfaces coated with the antimicrobial formulations effectively reduced the risk of cross-contamination of the fresh produce with hazardous bacteria in the simulated fresh produce-handing operation.

- Zein-based coating effectively reduced the microbial accumulation on SS harvesting knife during lettuce harvesting/trimming operations and on SS fruit sorting table during peach grading operations without affecting the quality of the fresh produce.

APPENDICES

Publications and Presentations

Publications

Doh, H., & Nitin, N. (2022). Gelatin-based rechargeable antibacterial hydrogel paint coating for reducing cross-contamination and biofilm formation on stainless steel. *Food Control*, *141*, 109113.

Huang, K., Yi, J., Young, G. M., & Nitin, N. (2022). Cell-based carriers incorporated antimicrobial coatings on diverse food contact surfaces for preventing cross-contamination of fresh produce. *Food Control*, *134*, 108700.

Presentations

Yi, J., & Nitin, N. (2021). Antimicrobial Food-Grade Coatings on Hydrophobic Plastics for Reducing Cross-Contamination of Fresh Produce. (v) *IAFP 2021*.

Budget Summary

The project was awarded $307,872 in grant funds, and most funds have been spent. Remaining funds will be used for travel to the June 2023 CPS Research Symposium.

Table 1 and Figures 1–28 (see below)

Table 1 Abbreviations used in the study

Abbreviation	Description
Bio-Mos and beeswax-based antimicrobial coating	
BM	Bio-Mos (Commercial yeast cell wall particles)
BM-EPL	Bio-Mos encapsulated with ε-poly-L-lysine
Gelatin-based hydrogel coating	
G(T)_x	Gelatin-tannic acid-coated stainless-steel knife. 'x' indicates the number of the coating layers.
G(T)_x@Cl	G(T)_x charged with chlorine.
Gel	Gelatin coating on the stainless steel
GelTA_x	Gelatin-tannic acid complex coating on the stainless steel
GelTA_x@Cl	Chlorine bound gelatin-tannic acid complex coating on the stainless steel
Zein and YC-based antimicrobial coating	
PP (or SS)	Polypropylene (or Stainless steel)
PP@Zein	PP coated with zein PP@Zein sprayed with YC
PP@Zein@YC	PP@Zein sprayed with YC
PP@Zein@YC@Cl	PP@Zein sprayed with chlorinated YC

(1) 'x' indicates the concentration (%) of tannic acid based on the gelatin content.

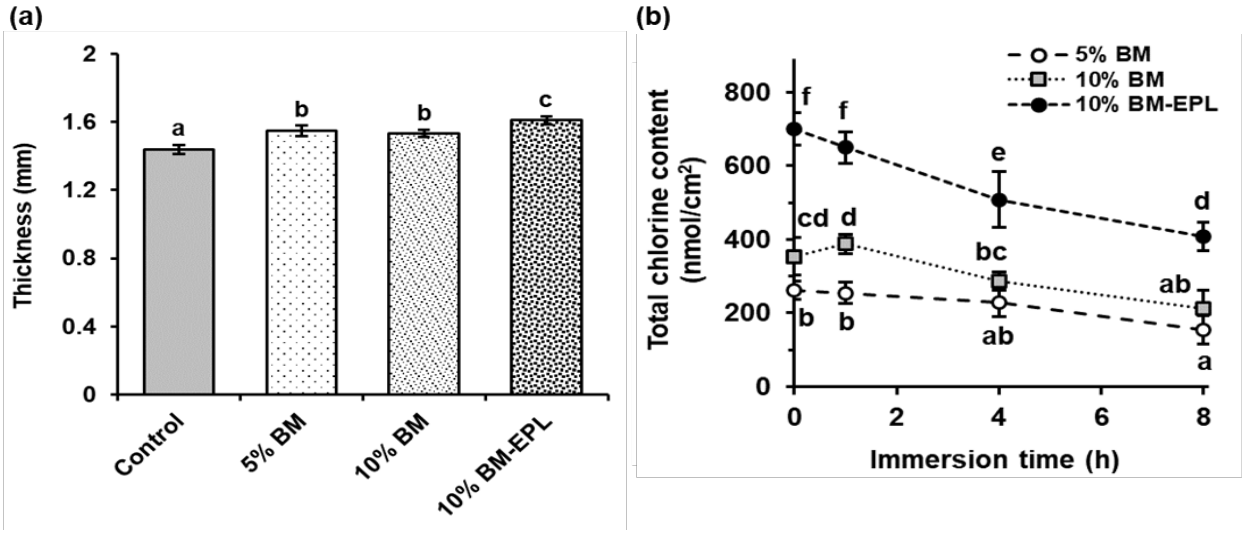

Figure 1. Properties of Bio-Mos/beeswax coatings on polypropylene plastic coupons: (a) The average thickness of uncoated/coated coupons; (b) chlorine stability of the Bio-Mos/beeswax coatings after water immersion for different times (0, 1, 4, 8 h). Control: uncoated coupons. 5% BM: coupons coated with a 5% Bio-Mos solution.10% BM: coupons coated with a 10% Bio-Mos solution. 10% BM-EPL: coupons coated with a 10% solution of Bio-Mos encapsulated with ε-poly-L-lysine.

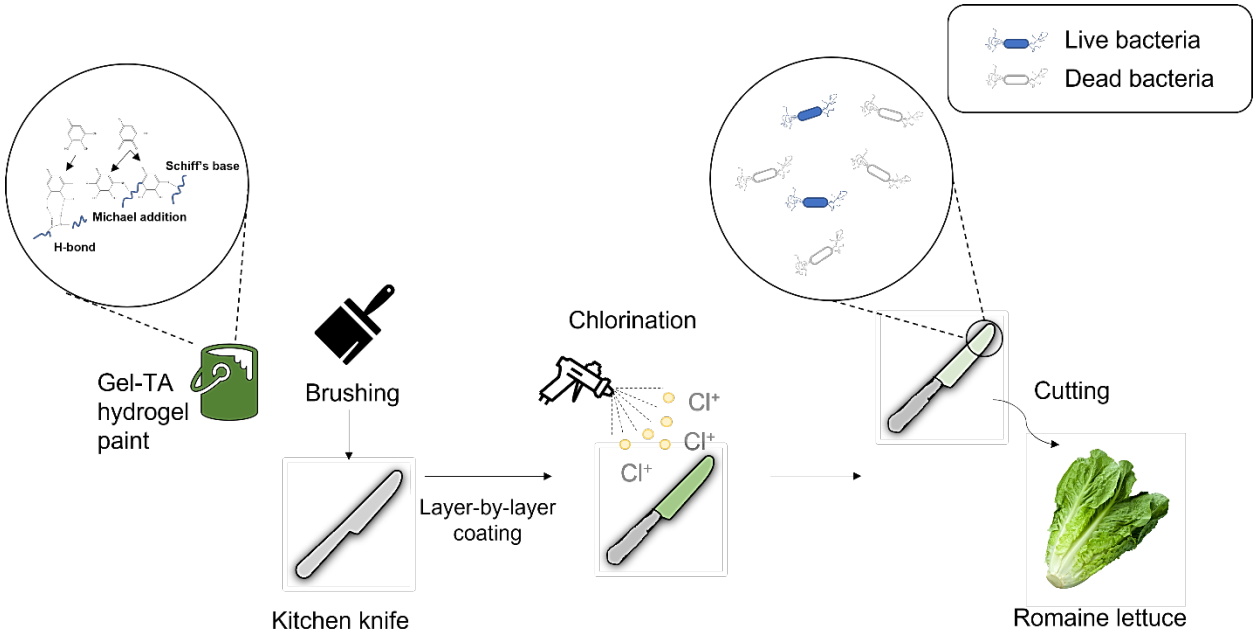

Figure 2. A schematic figure of the formulation and the antimicrobial application of the gelatin-tannic acid (TA) hydrogel coating on a stainless-steel knife.

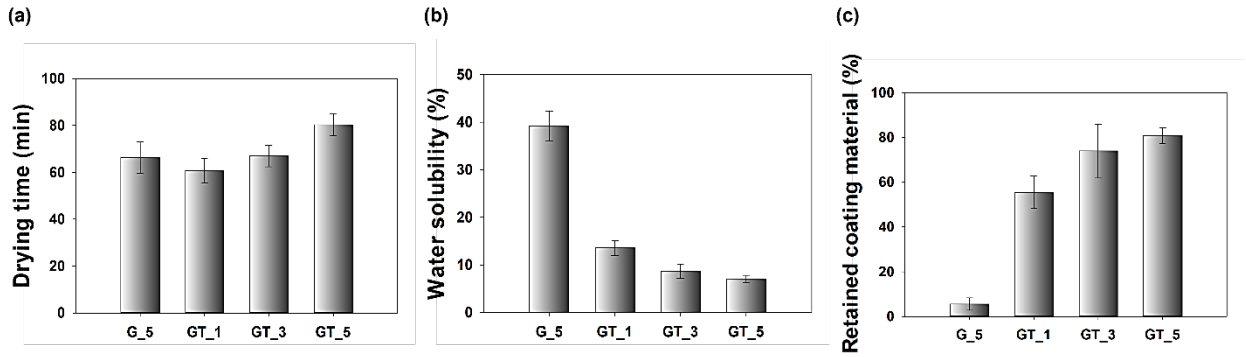

Figure 3. Characterization of the gelatin-TA hydrogel coating: (a) Drying time, (b) water solubility, and (c) resistance against the washing reagent (2% NaOH).

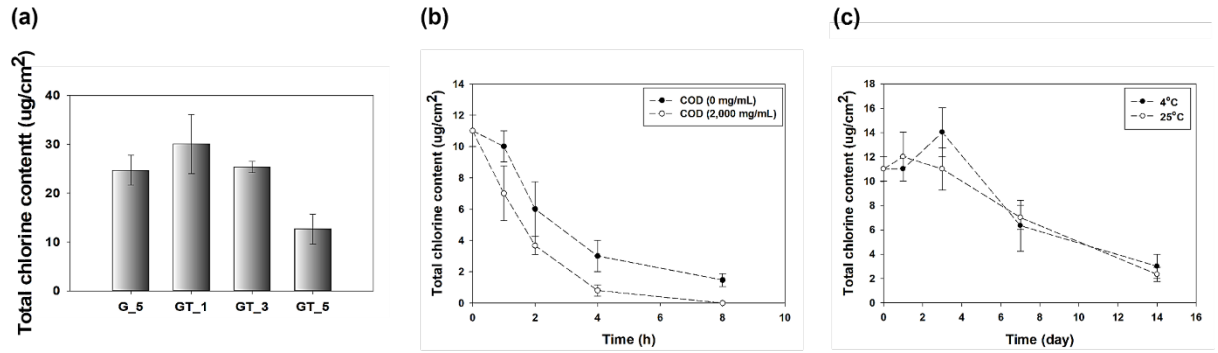

Figure 4. Stability of chlorine on gelatin-TA hydrogel coated stainless steel knife in diverse conditions: (a) Total active chlorine content, (b) in simulated wash water, and (c) at different storage temperatures.

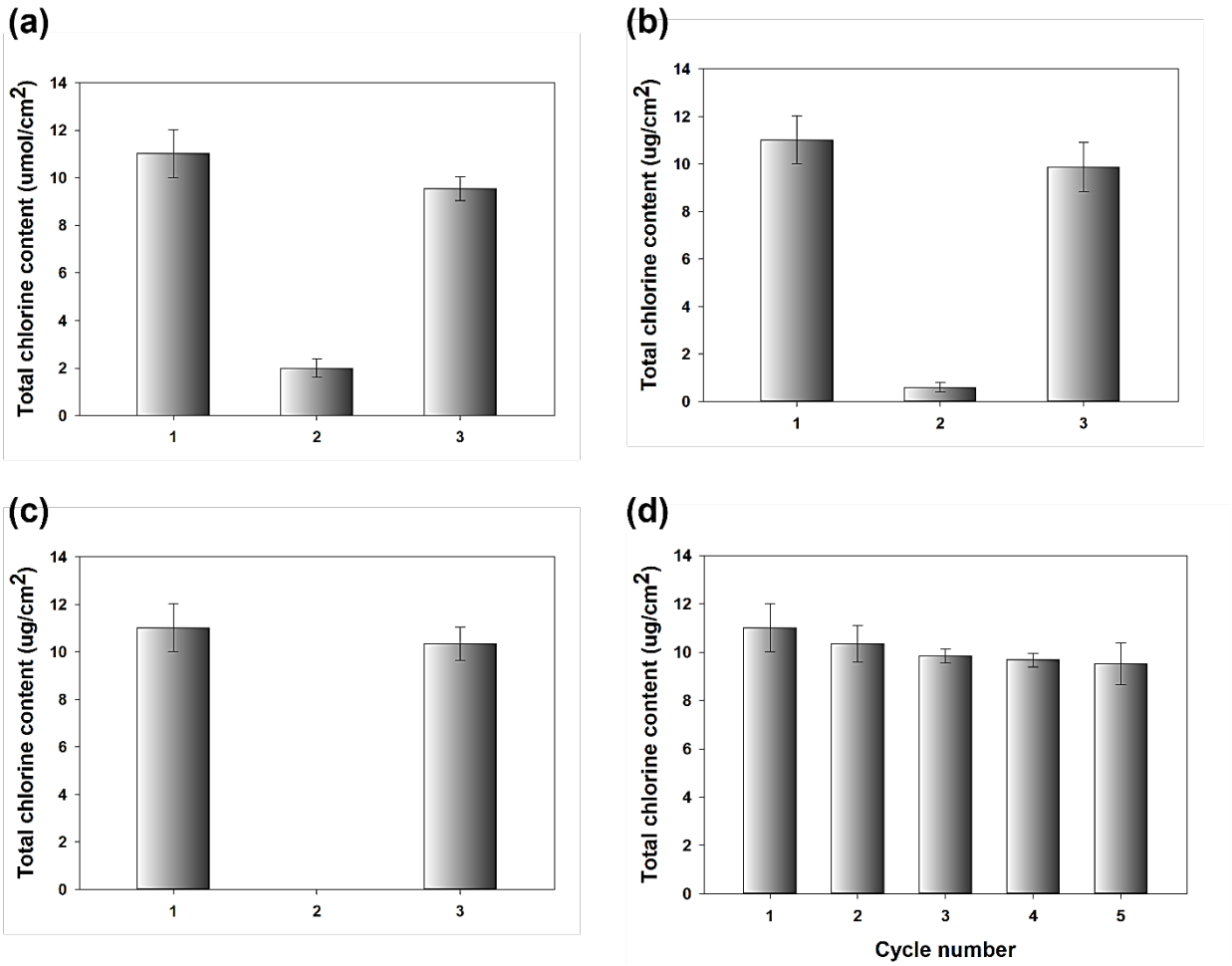

Figure 5. Rechargeability of chlorine on gelatin-TA hydrogel coated stainless steel knife after diverse quenching processes: After exposures to (a) extended storage at room temperature, (b) high organic matter (COD of 2,000 mg/L), (c) UV-A light, and (d) $Na_2S_2O_3$ for five cycles.

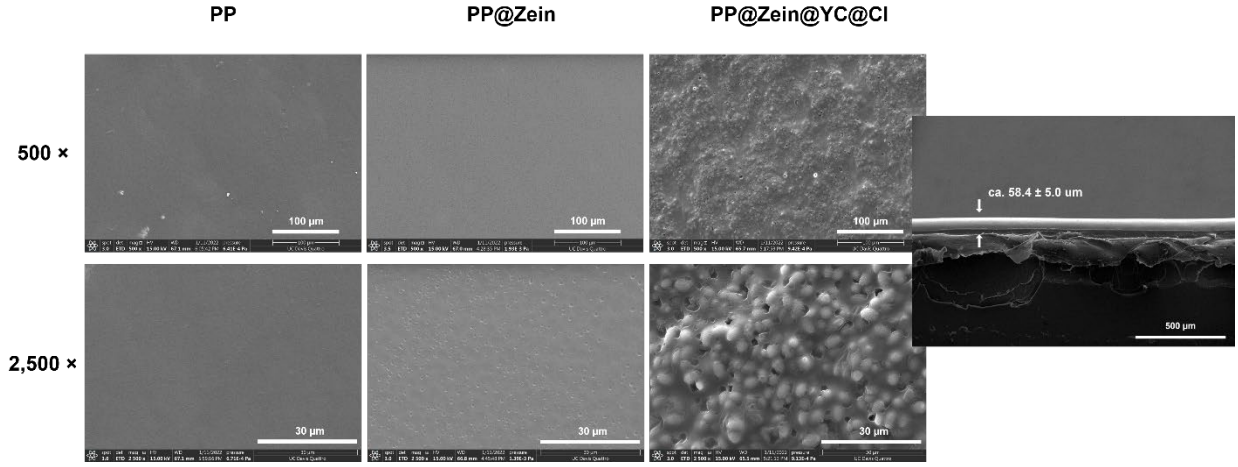

Figure 6. SEM images of the PP surfaces coated with zein and YC-based antimicrobial formulations.

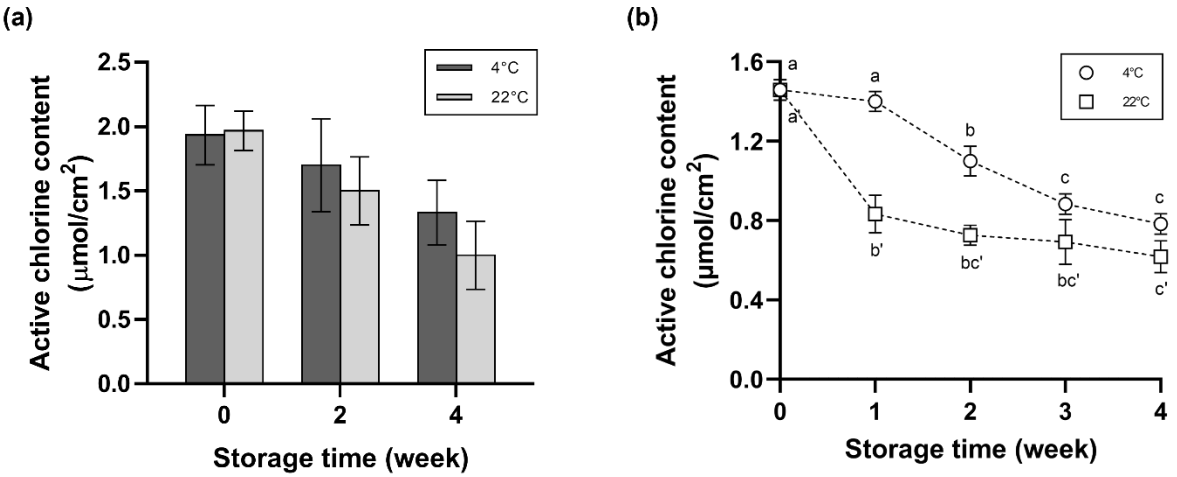

Figure 7. Storage stability of the zein and YC-based antimicrobial coating formed on (a) SS and (b) PP surfaces during 4 weeks of storage at 4°C and RT.

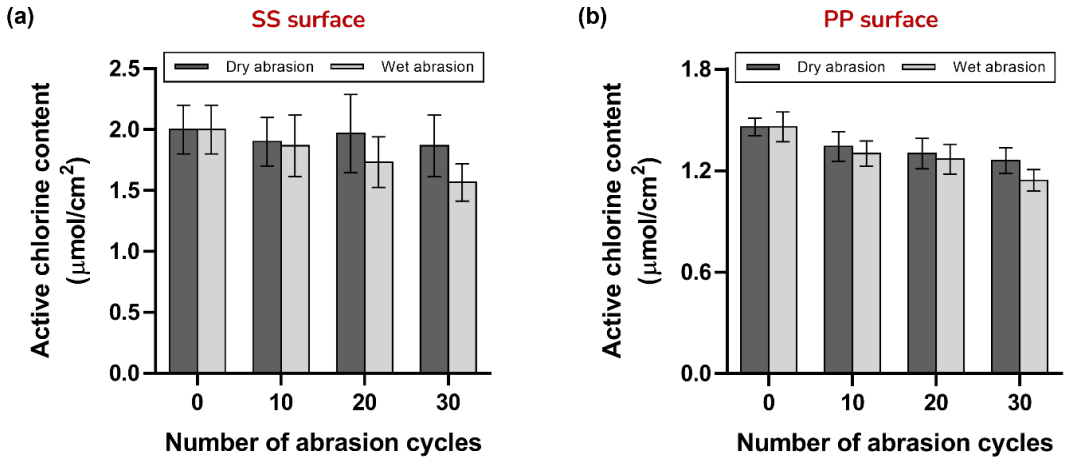

Figure 8. Mechanical resistance of the zein and YC-based antimicrobial coating against dry and wet shear abrasions on (a) SS and (b) PP surfaces (dry abrasion: 1 cycle = 16 single passes; wet abrasion: 1 cycle = 8 single passes; EPA-recommended method).

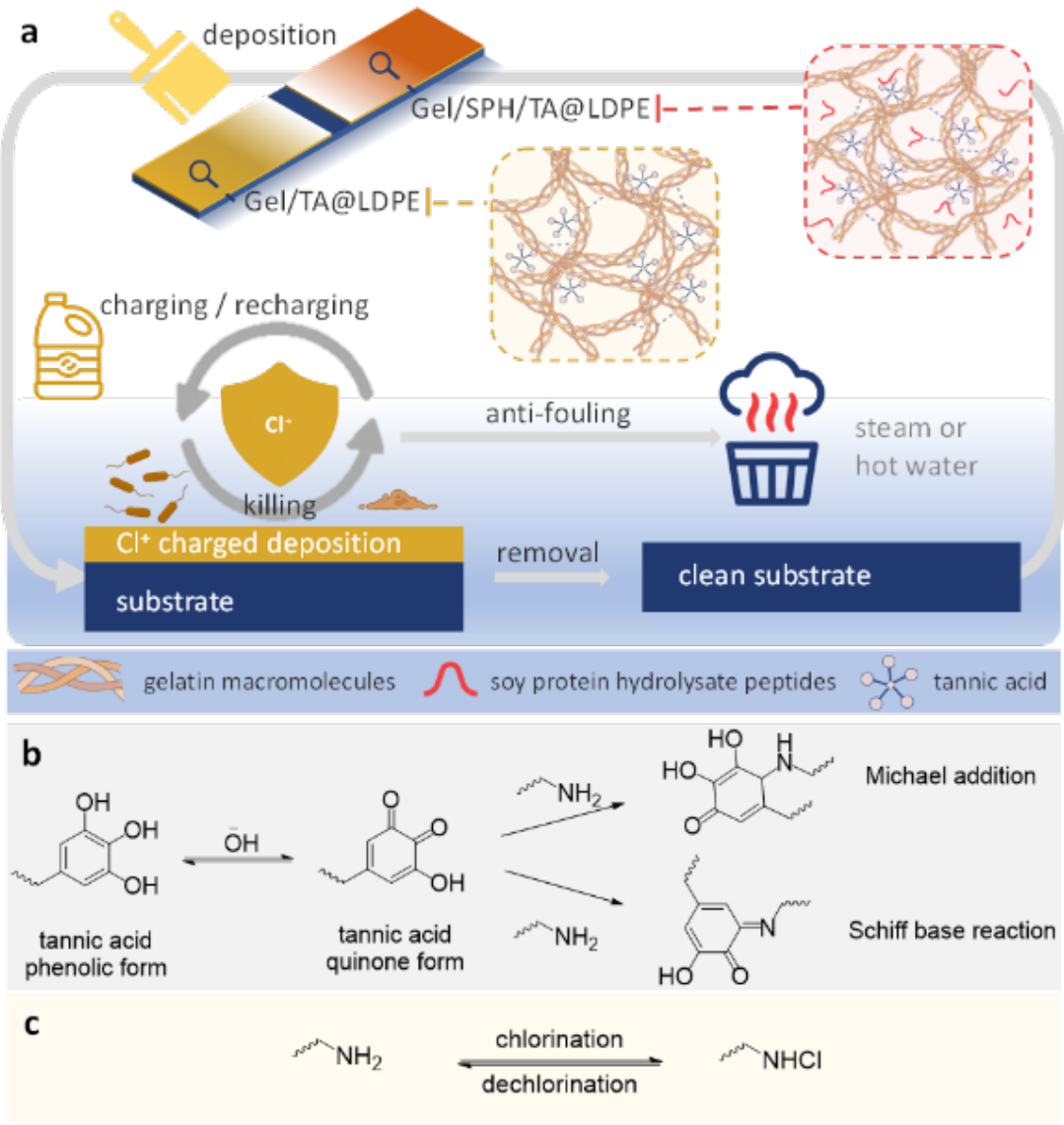

Figure 9. Schematics of Gel/TA@LDPE and Gel/SPH/TA@LDPE deposition systems in deposition development, structures of the Gel/TA@LDPE or Gel/SPH/TA@LDPE deposition layer, charging and recharging with active chlorine, bacterial killing, and anti-fouling functions, and removal after application (**a**). Crosslinking mechanism of employing tannic acid to crosslink proteins (**b**). The chlorination and dichlorination of the N-halamine precursors (**c**).

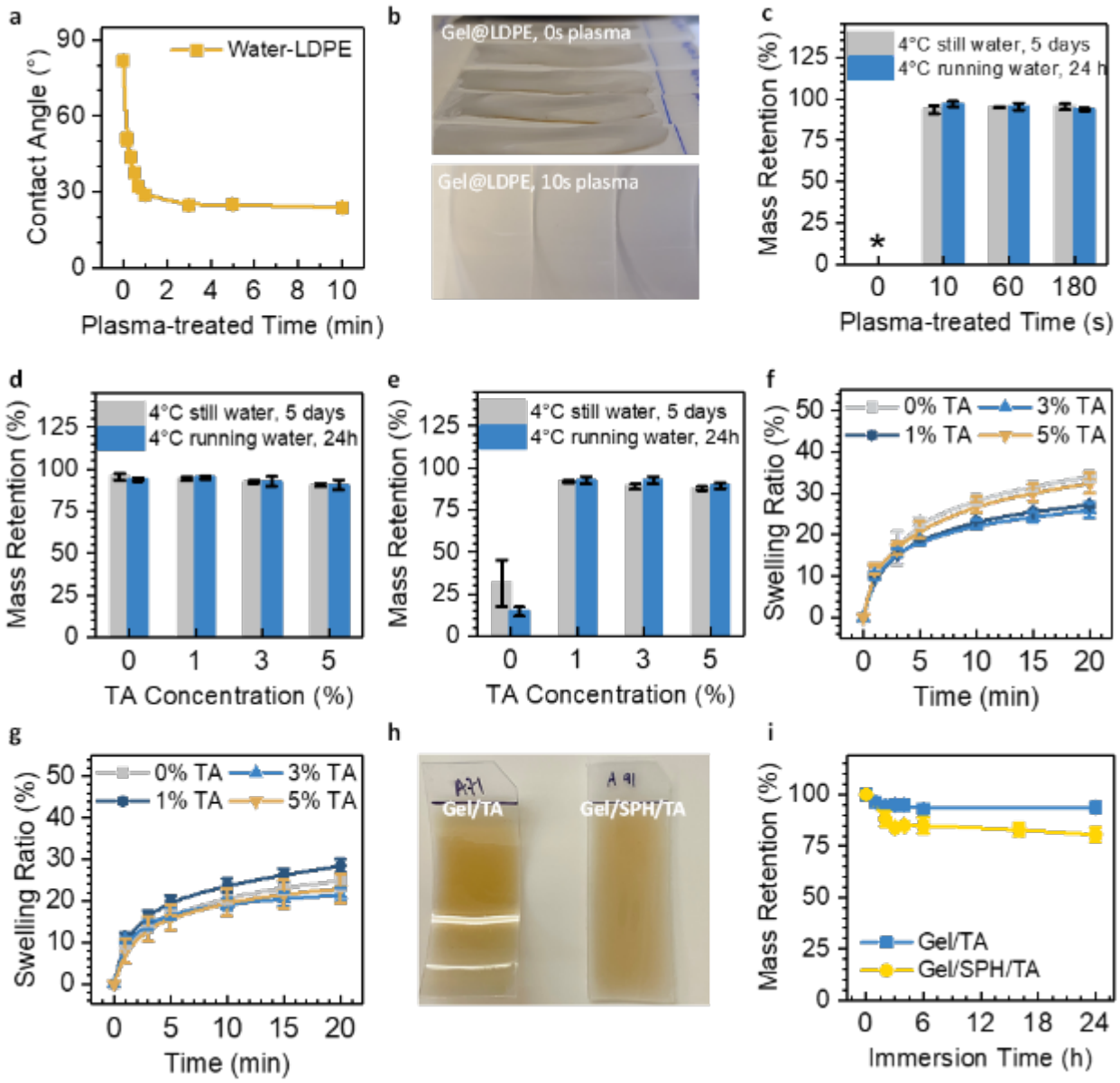

Figure 10. The change of water- LDPE contact angle along the increase of plasma treatment (**a**). Image of Gel@LDPE (10% gelatin) deposition on LDPE coupons with (bottom) or without (top) 10s plasma treatment (**b**). Mass changes of the Gel@LDPE deposition when coated LDPE coupons were immersed in a still water bath or shaking water bath at 4°C (**c**). Mass changes of the ratio of Gel-based (**d**) and Gel/SPH-based (**e**) deposition systems on LDPE coupons with a series of TA concentrations when immersed in a still water bath or shaking water bath at 4°C. The swelling ratio of Gel-based (**f**) and Gel/SPH-based (**g**) deposition systems with various TA concentrations at ambient conditions. The appearances of Gel/TA@LDPE and Gel/SPH/TA@LDPE-deposited LDPE coupons (**h**). The mass retention rate of Gel/TA@LDPE and Gel/SPH/TA@LDPE deposition when immersed in ambient condition water bath (**i**).

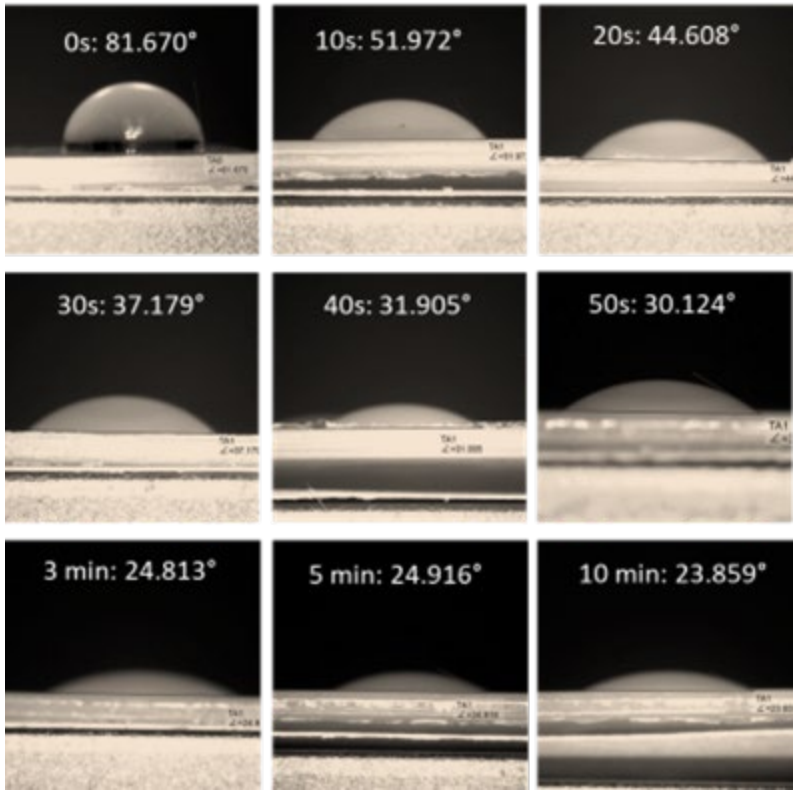

Figure 11. Images of water-LDPE contacting angle after 0 – 10 min of plasma treatment.

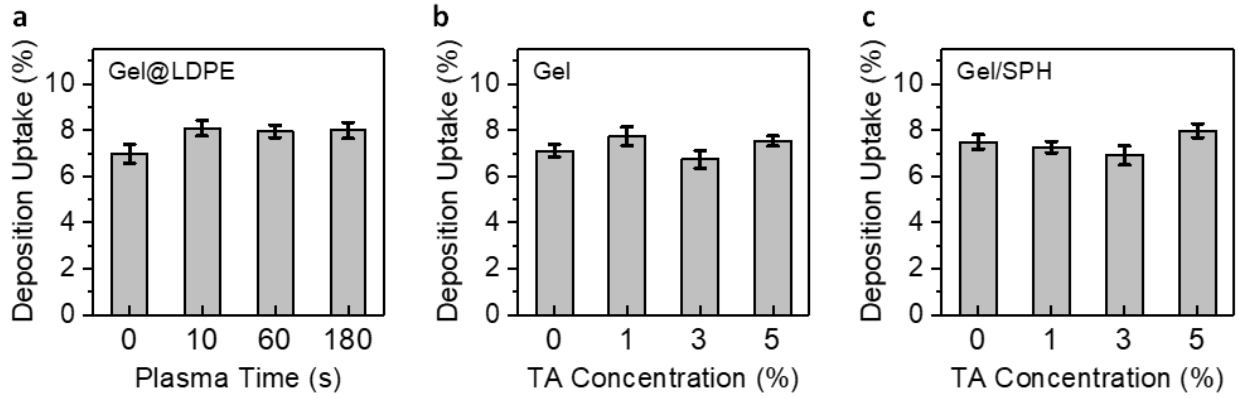

Figure 12. Pick-up rate of Gel (**a**), Gel-based (**b**), and Gel/SPH-based (**c**) deposition systems on LDPE coupons.

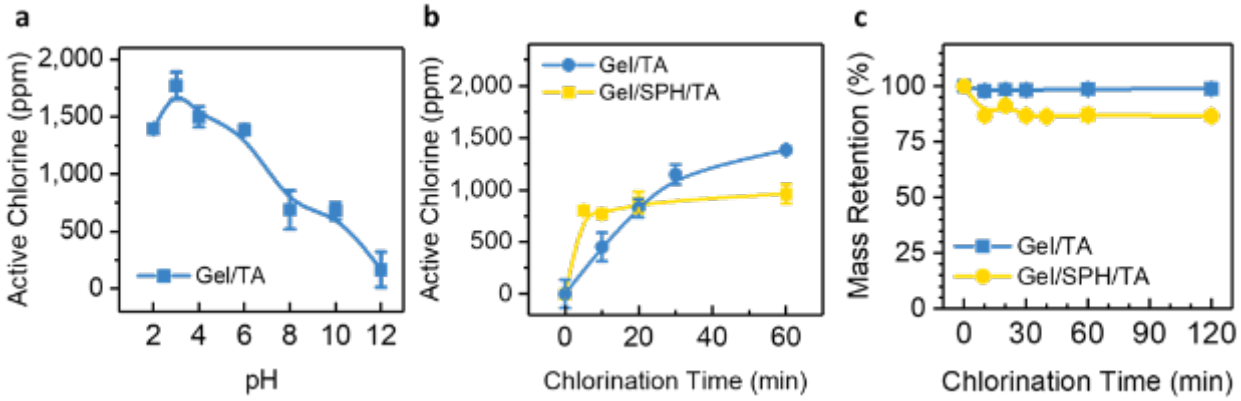

Figure 13. Active chlorine of Gel/TA@LDPE and Gel/SPH/TA@LDPE after being charged in chlorination solution with 10 ppm free active chlorine at different pH (**a**) and different duration (**b**). The mass retention rate of Gel/TA@LDPE and Gel/SPH/TA@LDPE when charged in chlorination solution (pH6, 10 ppm free active chlorine) for various times (**c**).

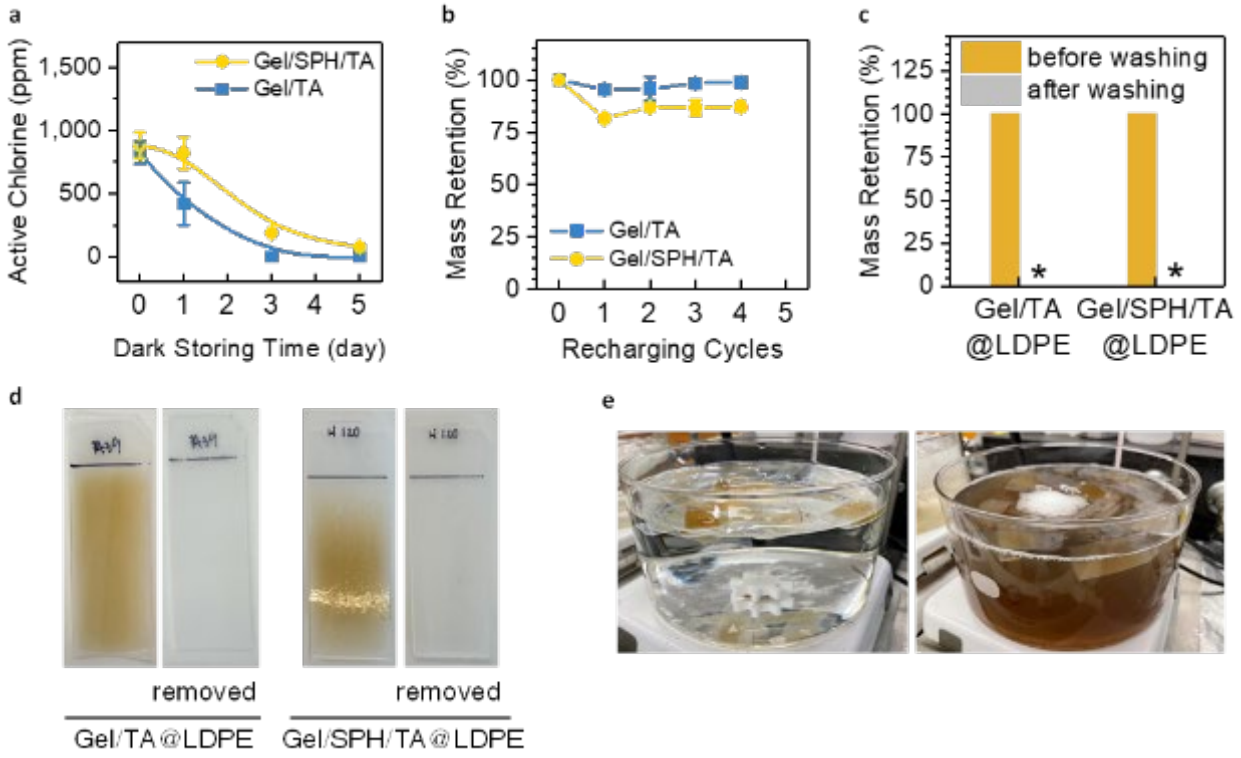

Figure 14. The stability of Cl^+ charged deposition systems against storage time (stored at 21°C, dark (**a**). Mass retention of Gel/TA@LDPE and Gel/SPH/TA@LDPE deposition systems along multiple chlorination cycles (**b**). Effectiveness of hot water removal towards both deposition systems, where star marks represent the mass after washing was below the detection limit (**c**). Images of LDPE coupons before and after hot water removal (**d**). The 50°C hot water bath before (left) and after (right) cleaning 250 pieces of Gel/TA@LDPE and Gel/SPH/TA@LDPE coated LDPE coupons (**e**).

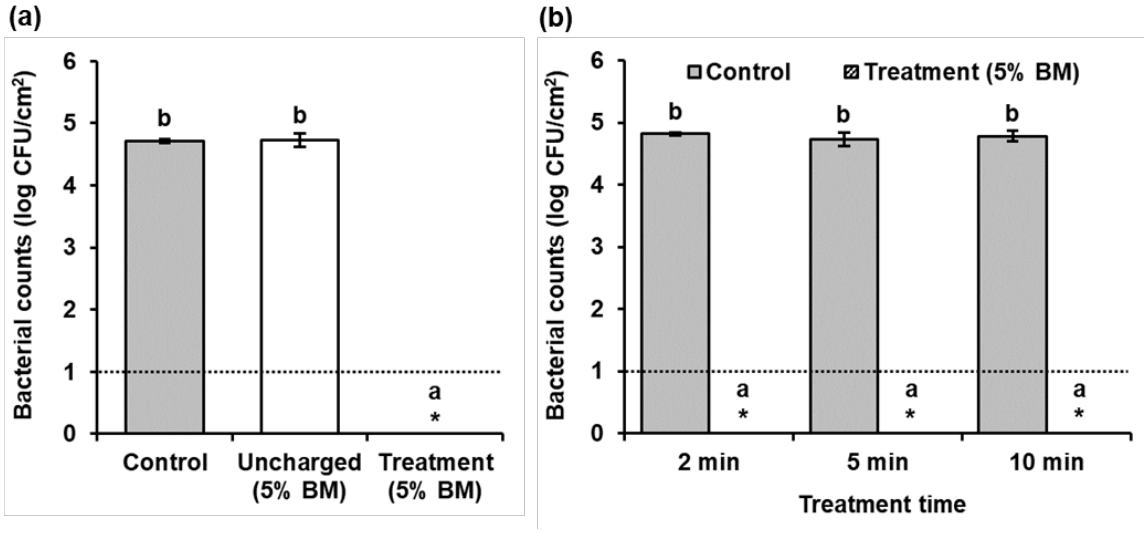

Figure 15. Antimicrobial activity of Bio-Mos/beeswax coatings on polypropylene plastic coupons. (**a**) Bacterial counts on each coupon 10 min after inoculation of *E. coli* O157:H7. (**b**) Bacterial reduction on the coated coupons for shorter treatment times (2, 5, 10 min). Control: uncoated coupons. Uncharged: coupons coated with a 5% Bio-Mos solution but uncharged with chlorine. 5% BM: coupons coated with a 5% Bio-Mos solution and then charged with 1% chlorine for 1 h.

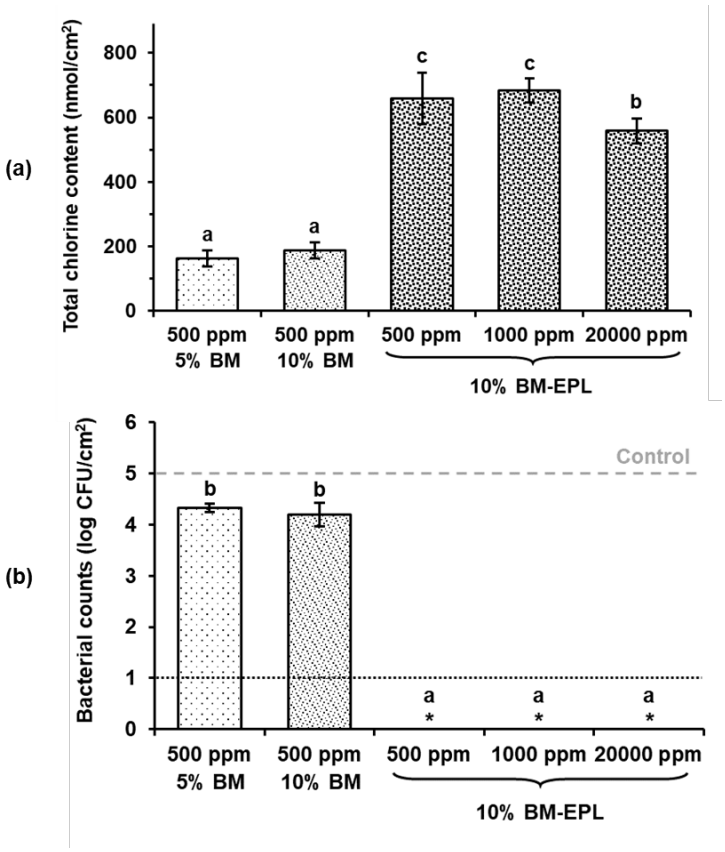

Figure 16. (**a**) Chlorine stability of the Bio-Mos/beeswax coatings on the presence of organic matter at different chemical oxygen demand levels (500, 1000, 20000 ppm) and (**b**) their respective antimicrobial activity against *E. coli* O157:H7 for 10 min treatment. Different letters indicate significant differences between values ($p < 0.05$), and the asterisks indicate that the bacterial counts were less than the limit of detection. The detection limit of the bacterial counts was 1 log CFU/cm^2, and the number of bacteria on the control coupon was 5 log CFU/cm^2.

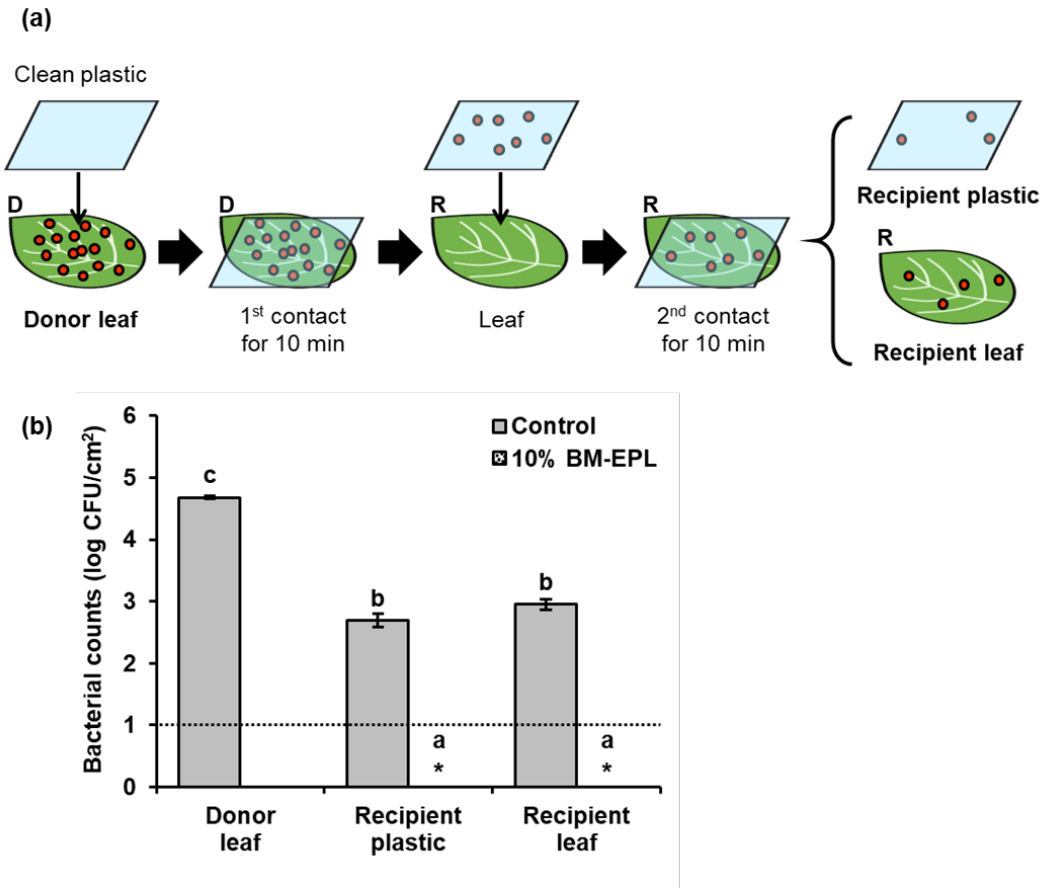

Figure 17. Effect of the Bio-Mos/beeswax coatings on reducing cross-contamination of fresh produce. (**a**) A schematic diagram of the simulated cross-contamination process. A leaf contaminated with *E. coli* O157:H7 and a clean plastic coupon were contacted for 10 min at an applied contact force of 1 N, and this resulting plastic coupon was used to contaminate a clean leaf. All samples were cut into the size of 1 × 1 cm^2. (**b**) Bacterial counts on the selected samples (donor leaf, recipient plastic/leaf). The results represent the mean values and their standard deviations (n = 3). Different letters indicate significant differences between values (p < 0.05), and the asterisks indicate that the bacterial counts were less than the limit of detection. The detection limit of the bacterial counts was 1 log CFU/cm^2.

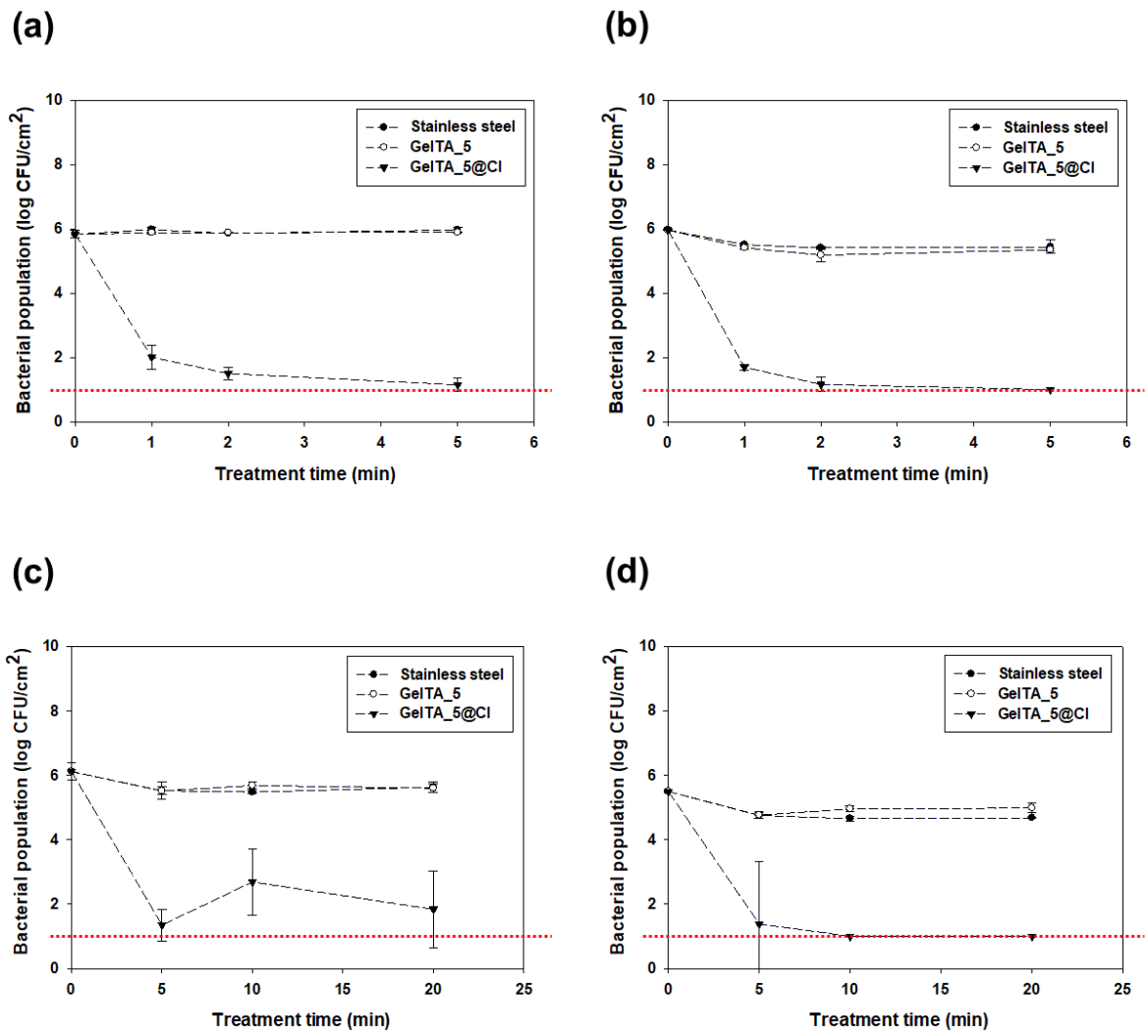

Figure 18. Antimicrobial activities against planktonic cells in DW (COD = 0 mg/L, [**a**, **b**]) and in the presence of organic content (COD = 2,000 mg/L, [**c**, **d**]). *Listeria innocua* (**a**, **c**) and *E. coli* O157:H7 (**b**, **d**). The horizontal dotted line indicates the theoretical detection limit (1.0 log CFU/cm^2) of the plate count method used in the study.

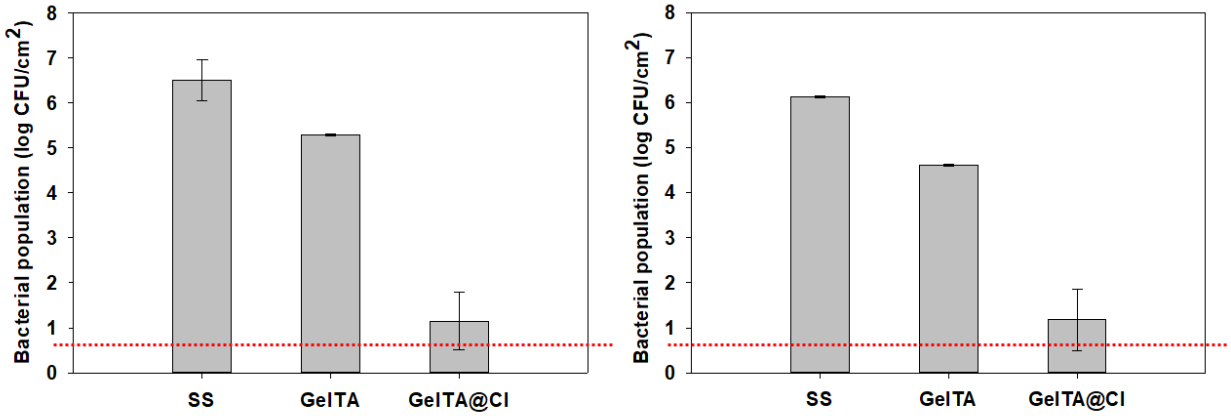

Figure 19. Anti-biofouling activities of the gelatin-based hydrogel coating against *L. innocua* (left) and *E. coli* O157:H7 (right). The horizontal dotted line indicates the theoretical detection limit (0.84 log CFU/cm^2) of the plate count method used in the study.

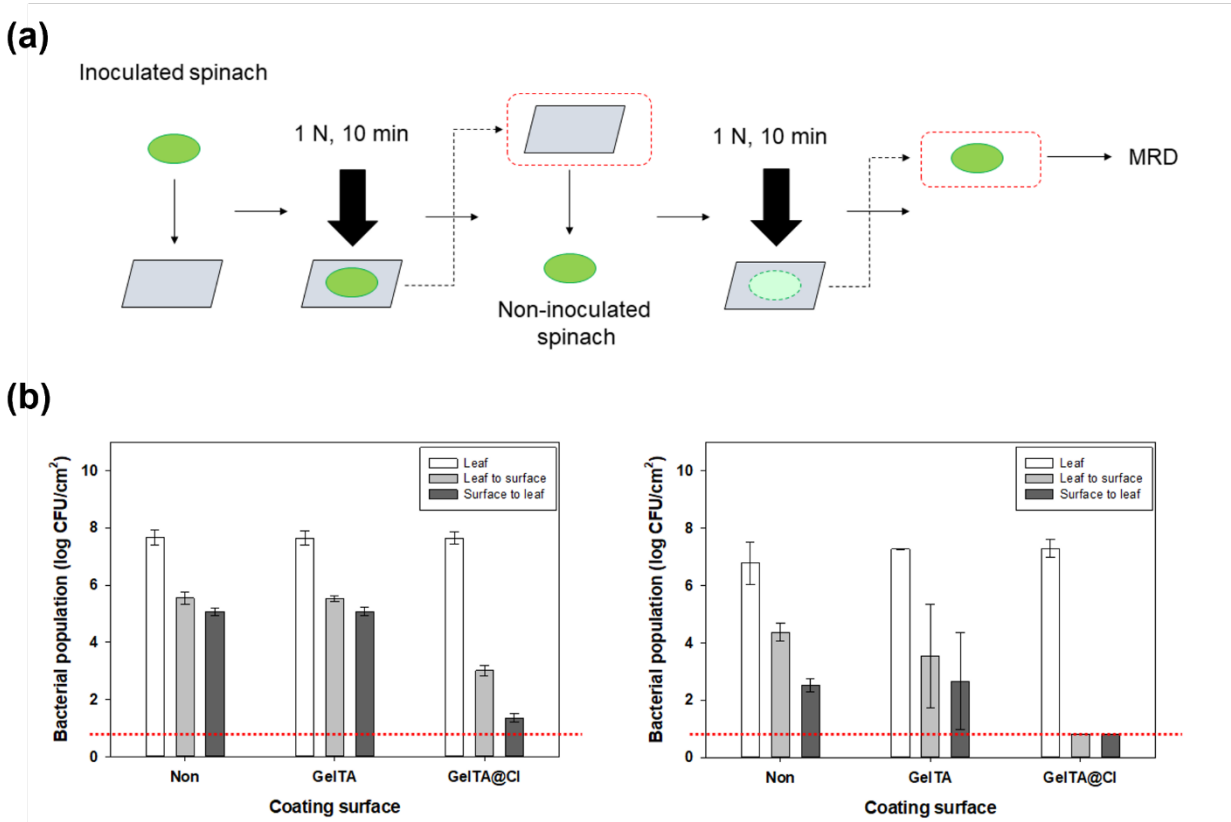

Figure 20. Leaf-surface-leaf cross-contamination study on Gel-TA hydrogel coating: (**a**) A schematic of the simulated cross-contamination process; (**b**) bacterial populations of *L. innocua* (left) and *E. coli* O157:H7 (right) on donor leaf, SS surface, and recipient leaf. 'Non' indicates non-coated stainless steel. The detection limit of the plate count method used in the study is indicated as a horizontal dotted line (0.84 log CFU/cm^2).

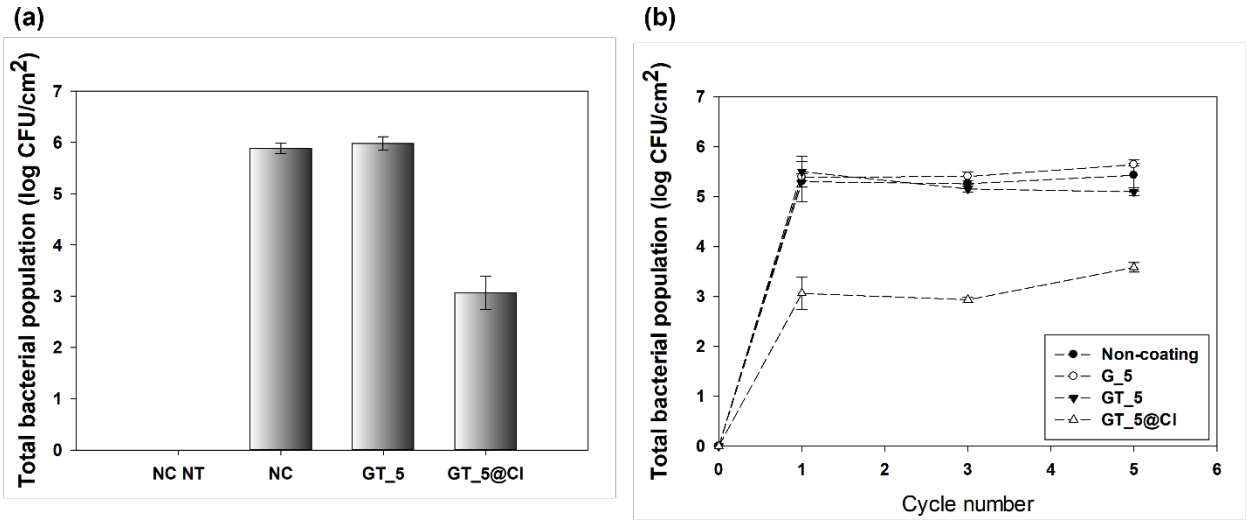

Figure 21. Antimicrobial activities of G(T)_5@Cl against the natural microflora present on the fresh Romaine lettuce: (a) after the first chopping cycle and (b) during the five chopping cycles (30 choppings = 1 cycle).

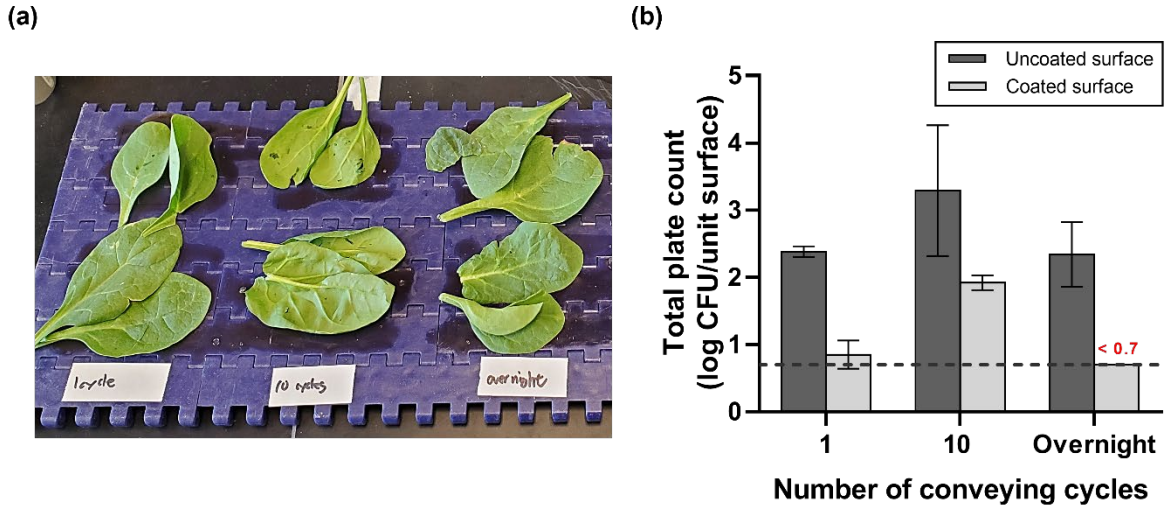

Figure 22. Effectiveness of the gelatin-based antimicrobial coating in preventing leaf-to-surface bacterial cross-contamination on the actual plastic conveyor belt (1 conveying cycle = 10 min incubation).

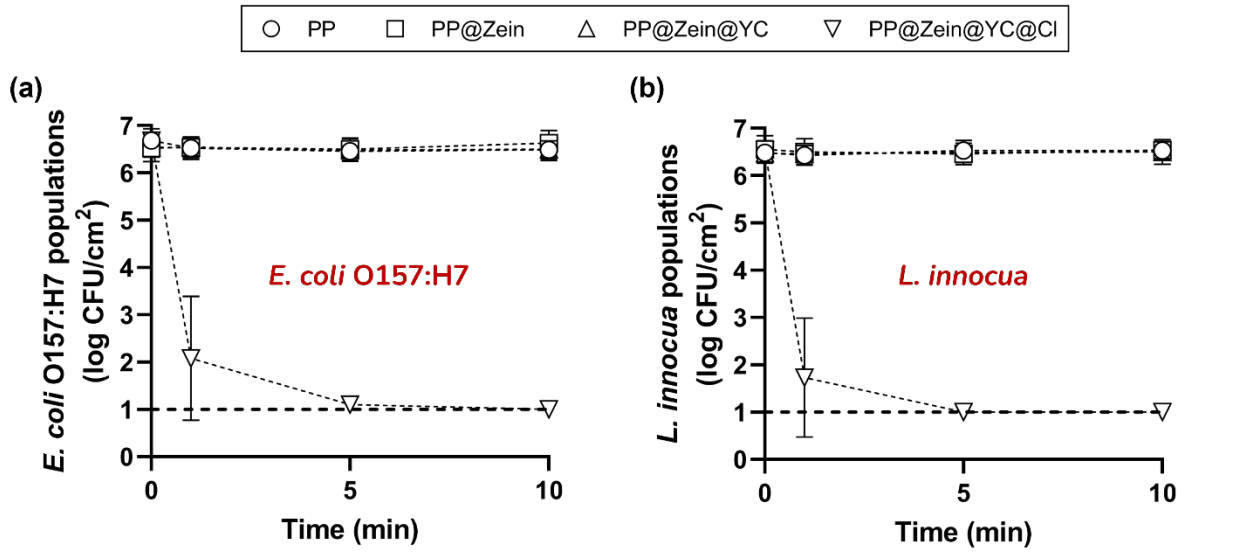

Figure 23. Antimicrobial activities of the zein and YC-based coating formed on PP surfaces against (a) *E. coli* O157:H7 and (b) *L. innocua*.

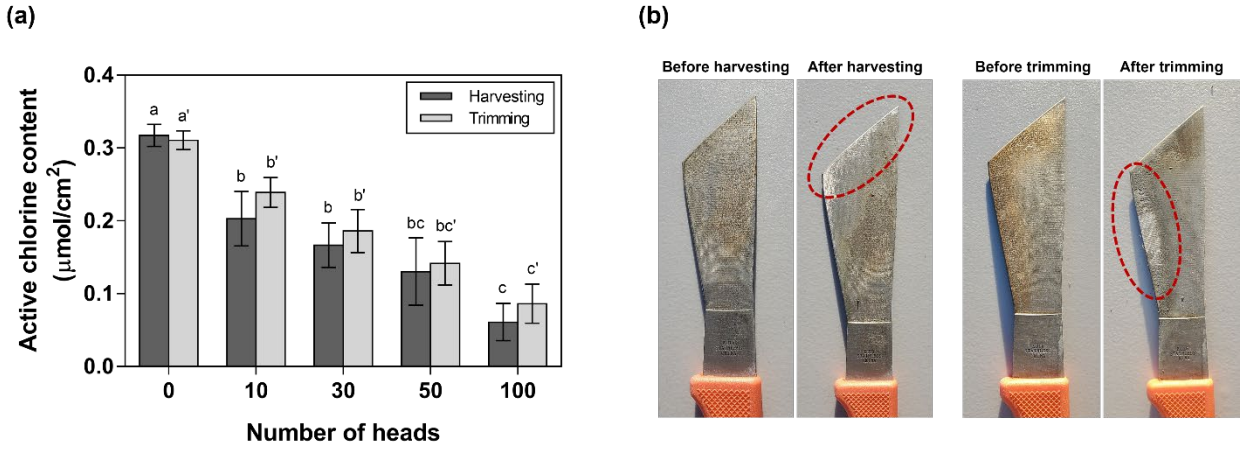

Figure 24. A field test performed with a lettuce harvesting knife coated with zein and YC-based formulation: (a) Change in active chlorine contents and (b) images of the coated knife before and after harvesting/trimming 100 heads of lettuce.

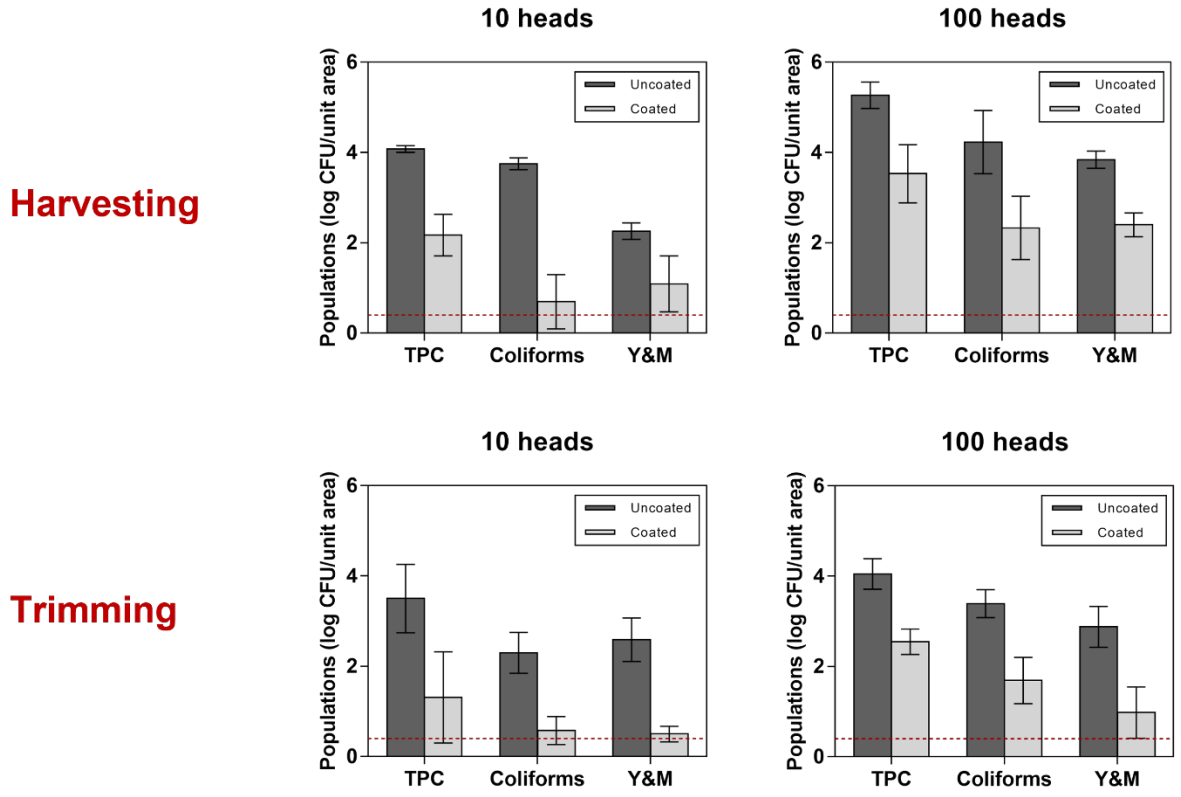

Figure 25. Antimicrobial activities of the harvesting knife with and without zein-based antimicrobial formulations during harvesting (upper) and trimming (lower) 100 heads of lettuce.

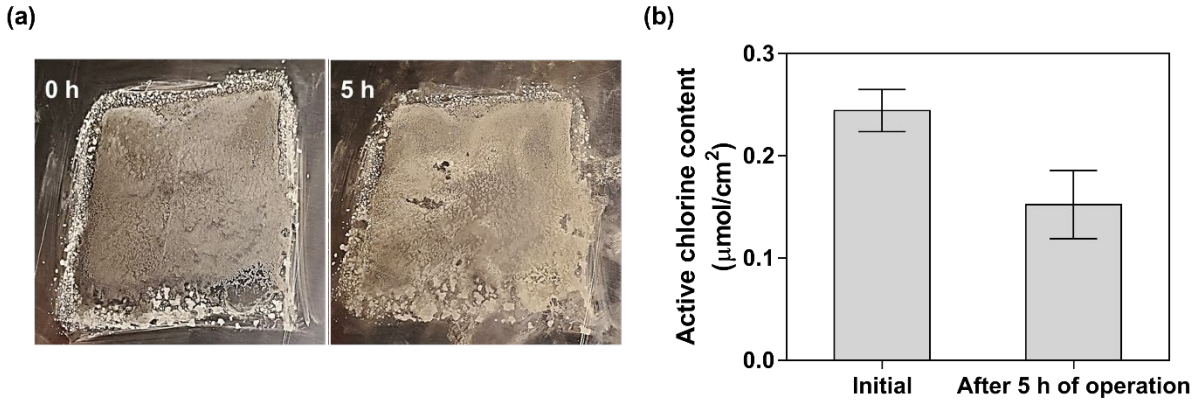

Figure 26. A field test performed on a stone fruit sorting table using zein and YC-based coating formulation: (a) images of the coated surfaces and (b) change in active chlorine contents of the coated surfaces before and after 5 h of the peach grading operation.

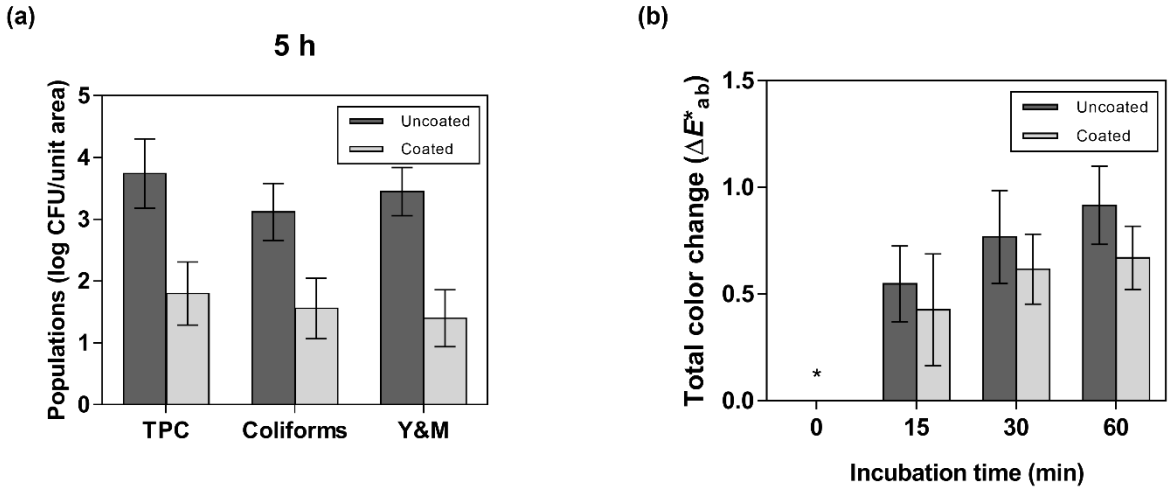

Figure 27. A field test performed on a stone fruit sorting table using zein and YC-based coating formulation: (a) antimicrobial activities of the sorting table with and without zein-based antimicrobial formulations during five hours of peach grading operation; (b) Total color change (ΔE^*_{ab}) of the peach samples rolled on the coated surfaces for 60 min.

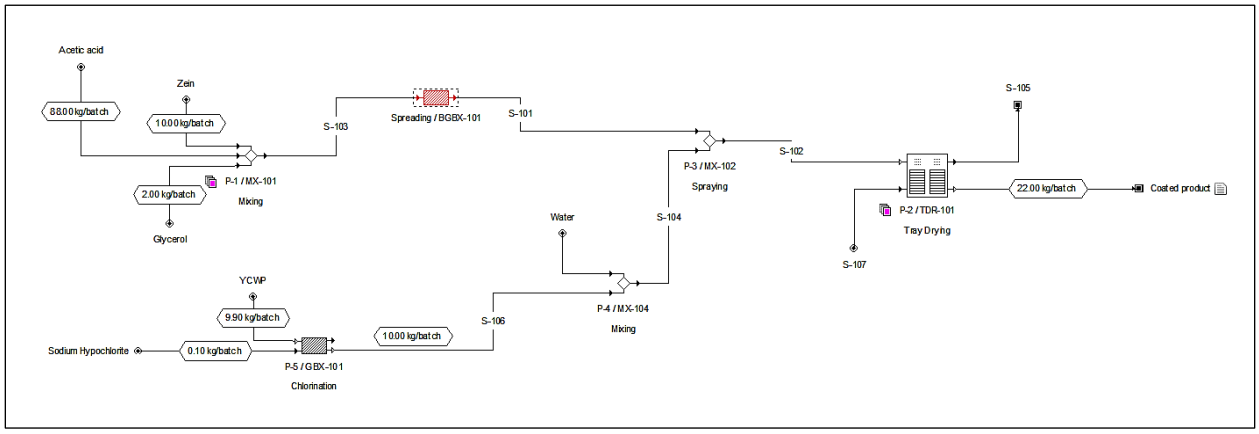

Figure 28. Schematic diagram of an industrial-scale, zein-based coating formulation process.

References cited

1. Tang, Songsong, Guoqiang Chen, and Gang Sun. "Computer-Assisted Design of Environmentally Friendly and Light-Stable Fluorescent Dyes for Textile Applications." *International Journal of Molecular Sciences* 20.23 (2019): 5971.
2. Peixin Tang, Mengxiao Zhang, Bolin Ji, Teera Yong, Gang Sun, Hierarchical Nucleophilic Nanofibrous Membranes for Fast, Durable, and Bare-Eye Visible Detoxification of Carcinogenic Alkylating Toxicants, *Advanced Functional Materials*, 2019, 29. 1905990.
3. Yuan Yu, Peixing Tang, Bogdan Barnych, Cunyi Zhao, Gang Sun, Mingqiao Ge, Design and Synthesis of Core–Shell Carbon Polymer Dots with Highly Stable Fluorescence in Polymeric Materials, *ACS Applied Nano Materials* 2 (10), 6503-6512.
4. Kai Liu, Kelu Yan, Gang Sun, Mechanism of H2O2/bleach activators and related factors, *Cellulose* 26 (4), 2743-2757.
5. Zehong Wang, Yang Si, Cunyi Zhao, Dan Yu, Wei Wang, Gang Sun, Flexible and Washable Poly (Ionic Liquid) Nanofibrous Membrane with Moisture Proof Pressure Sensing for Real-Life Wearable Electronics, *ACS applied materials & interfaces* 11 (30), 27200-27209.
6. Tang, Peixin, Ngoc Thi-Hong Nguyen, Jeane Gladys Lo, and Gang Sun. "Colorimetric Detection of Carcinogenic Alkylating Fumigants on Nylon 6 Nanofibrous Membrane. Part II: Self-Catalysis of 2-Diethylaminoethyl Modified Sensor Matrix for Improvement of Sensitivity." *ACS applied materials & interfaces* (2019). *1* (14), pp 13632–13641
7. Tang, Songsong, Cunyi Zhao, Guoqiang Chen, and Gang Sun. "A study on computerized selection of fluorescent dyes for environmentally friendly textile applications." *Dyes and Pigments* 165 (2019): 256-263.
8. Shixiong Yi, Yushan Zuo, Sheng Sun, Fangyin Dai, Yang Si, Gang Sun, Rechargeable Photoactive Silk-Derived Nanofibrous Membranes for Degradation of Reactive Red 195, *ACS Sustainable Chem. Eng.*, 2019, *7* (1), pp 986–993.
9. Peixin Tang, Maria Trinidad Gomez, Ho Ting Leung, Gang Sun, 2019. Bio-inspired ultrasensitive colorimetric detection of methyl isothiocyanate on nylon-6 nanofibrous membrane: A comparison of biological thiol reactivities. *J. of Hazardous Materials*, *362*, pp.375-382.
10. Ahmed Y El-Moghazy, Cunyi Zhao, Georges Istamboulie, Noha Amaly, Yang Si, Thierry Noguer, Gang Sun, 2018. Ultrasensitive label-free electrochemical immunosensor based on PVA-*co*-PE nanofibrous membrane for the detection of chloramphenicol residues in milk, *Biosensors and Bioelectronics,* 117, 838-844.
11. Maryam Tamizifar and Gang Sun, Surface modification of poly (ethylene terephthalate) fibers via controlled radical graft polymerization. *J. of Applied Polymer Science*, *135*(11).
12. Peixin Tang and Gang Sun, 2018.Highly sensitive colorimetric paper sensor for methyl isothiocyanate (MITC): Using its toxicological reaction, *Sensors & Actuators: B. Chemical*, 261, 178-187.
13. Peixin Tang, Ho Ting Leung, Maria Trinidad Gomez, Gang Sun, Sensitivity-tunable Colorimetric Detection of Chloropicrin Vapor on Nylon-6 Nanofibrous Membrane Based on a Detoxification Reaction with Biological Thiols. *ACS sensors* 2018, *3* (4), pp 858–866.
14. Yue Ma, Danjie Zhu, Yang Si, and Gang Sun, 2018. Fabricating Durable, Fluoride-Free, Water Repellency Cotton Fabrics with CPDMS*, J. of Applied Polymer Science, 135*, 46396.
15. Huang, K., Yi, J., Young, G. M., & Nitin, N. (2022). Cell-based carriers incorporated antimicrobial coatings on diverse food contact surfaces for preventing cross-contamination of fresh produce. *Food Control*, *134*, 108700.
16. Doh, H., & Nitin, N. (2022). Gelatin-based rechargeable antibacterial hydrogel paint coating for reducing cross-contamination and biofilm formation on stainless steel. *Food Control*, *141*, 109113.